Point-on-Wave Switching for Distribution Transformer Inrush Current Reduction

Saravan Khumar Ravichandran

Department of Electrical & Computer Engineering

McGill University, Montreal, Canada

June 2015

A thesis submitted to McGill University in partial fulfillment of the requirements for the degree of Master of Engineering in Electrical Engineering

Abstract

Inrush transients can have highly undesirable effects on the distribution transformers and are due to core flux asymmetry during energization. These inrush currents can be of very high magnitude, harmonic rich which can harm the transformer itself and mal-operate the protective device operation. Several methods are used to reduce their magnitude such as closing resistors, reduction of residual flux magnitudes, and controlled switching. Selecting any one of those methods is a decision that must factor-in cost-effectiveness and ease of implementation. Significant advances in switchgear development, during the past decades, have shifted interest towards point-on-wave controlled-switching oriented techniques.

This thesis investigates the methodology of simultaneous controlled point-on-wave switching for lower cost range distribution transformers which cannot afford circuit breakers with independent pole control. The investigation is simulation-based and a simple switching rule of thumb and an analytical optimization method are deduced from brute force search approach that involves a series of energization simulations using actual field data. This rule can be easily implemented and is shown that they can substantially reduce inrush currents as opposed to random energization.

The simulations are carried out in the SIMULINK SimPowerSystems environment but reference to EMTP-RV results is also made for comparison. Transformer core models of different magnetic characteristics and geometrical configurations are used. So are different three-phase winding connections to assess the effectiveness of the examined approach.

Résumé

Les transitoires d’afflux peuvent avoir des effets hautement indésirables sur les transformateurs de distribution et sont dues à l'asymétrie du flux noyau pendant l'excitation. Ces courants d'afflux peuvent être de très grande ampleur, peut être riche en harmonique, peut nuire le transformateur lui-même et bouleverser l'opération de protection de l'appareil. Plusieurs méthodes sont utilisées pour réduire l'ampleur telle que des résistances de fermeture, la réduction des amplitudes de flux résiduel, et la commutation contrôlée. La sélection de l'une de ces méthodes est une décision qui doit tenir compte du coût-efficacité et de la facilité de mise en œuvre. Au cours des dernières décennies, des progrès significatifs dans le développement de l'appareillage ont déplacé l'intérêt vers le point sur les techniques orientées des ondes contrôlées par commutation.

Cette thèse étudie la méthodologie de commutation contrôlée sur point d’onde simultanée pour des transformateurs de distribution à moindre coût qui n’ont pas de disjoncteurs avec contrôle indépendant de pôle. L'enquête est basée sur la simulation et les règles de commutation de base simples et une méthode d’optimisation analytique sont déduites des approches de recherche par la force brute qui impliquent une série de simulations d'excitation en utilisant des données réelles. Cette règle peut être facilement mise en œuvre et il est démontré qu'elle peut réduire de manière conséquente les courants d'appel, par opposition à l'excitation aléatoire.

Les simulations sont réalisées dans l'environnement SIMULINK SimPowerSystems mais la référence aux résultats EMTP-RV est également faite pour la comparaison. Des modèles de noyau de transformateur de différentes caractéristiques magnétiques et configurations géométriques, ainsi que différentes connexions sinueuses triphasés sont utilisés pour évaluer l'efficacité de l'approche examinée.

Acknowledgements

I would like to sincerely thank my supervisor, Professor Géza Joós, for his guidance and support throughout my Master's studies. I am extremely grateful for the opportunities that he has provided me and allowed me to pursue. I am thankful to him for giving me a chance to learn, understand and improve my knowledge in power systems engineering.

I would like to express my gratitude to Dr. Anthony J Rodolakis and Dr. Khalil El-Arroudi for their continued support in helping me understand power system protection in a more profound manner. Their advices played a vital role in my research and I thank them for providing assistance in editing the manuscript of this thesis. I thank Mr. Aziz Ijdir from Vizimax Inc., for taking time to explain in detail about the industrial practices in transformer switching as well as providing the field measurement data for the simulations. I also thank Michael Ross for giving me an insight into this topic and for providing me the simulation results from EMTP RV. I would like to thank all my colleagues in the Electric Energy Systems Laboratory group. In particular, my heartfelt thanks to Subhadeep Bhattacharya and Syed Qaseem Ali for giving me valuable advice and support towards improving my research. I would like to acknowledge Diego Mascarella and Michael Ross for their support in writing the French version of the abstract.

I am greatly thankful to my parents and my sister, Vidya for their endless love, support and encouragement. Be it a moment of happiness or crisis their motivation drove me ahead. To my friends here in Montreal, Yogesh, Balaji, Mohana, Poulami, Debi Prasad, Rohini, Rishabh, Dipannita, to my colleagues Shijia Li, Harmeet Cheema, Qiushi Cui, Mike Quashie and to my friends in Chennai, Rajiv, Raja, Ram, Zaheer, Sharath, Selva, Saravanan, Sathiya, Satheesh, Saranya, Shyama, Uma, Varshinee, Poornima and everyone I have missed here, thank you for your support and encouragement.

The financial support provided by McGill University and the NSERC/Hydro-Québec Industrial Research Chair on the Integration of Renewable Energies and Distributed Generation into the Electric Distribution Grid held by Professor Géza Joós is acknowledged.

Contents

List of Figures

List of Tables

List of Acronyms

IC	Inrush Current
DC	Direct Current
LV	Low Voltage
HV	High Voltage
HVDC	High Voltage Direct Current
EMTP-RV	Electro Magnetic Transient Program-Restructured Version
RDDS	Rate of Decrease of Dielectric Strength

List of Symbols

ω	Angular Frequency (rad)
$v(t)$	induced voltage across the winding (V)
$\varphi(t)$	Flux through the winding (Vs)
V	Peak Voltage magnitude (V)
φ_{max}	Maximum flux (Vs)
N	Number of turns in Primary Winding of the transformer
φ_R	Residual Flux (Vs)
t_{op}	Optimal closing time instant
$\theta_o, theta\_open$	Opening Angle (deg)
$\theta_c, theta\_close$	Closing Angle (deg)
$\Delta\theta, delta\_theta$	Difference between Opening angle and Closing angle (deg)
Y_g	Wye grounded winding of transformer
$Ɽ_{Leg}$	Reluctance of core limb (At/Wb)
$Ɽ_{Yoke}$	Reluctance of yoke (At/Wb)
$Ɽ_0$	Reluctance of air gap (At/Wb)
$Ɽ_{Lhv}$	Leakage reluctance of high voltage winding (At/Wb)
$Ɽ_{Llv}$	Leakage reluctance of low voltage winding (At/Wb)

Chapter 1 Introduction

1.1 Background

Power transformers rely on the magnetic circuits formed by ferromagnetic core(s) to ensure effective magnetic flux linkage between their windings. The typically used soft ferrous alloy materials to construct the transformer cores have magnetic performance characteristics that include hysteresis and saturation. Virtually all power transformers are normally operated below, but close to, the saturation level of their core magnetization curve for economic reasons.

Whenever a transformer is de-energized, there is residual flux remaining in the core due to the hysteresis phenomenon. The resulting power frequency core flux will, upon energization, be generally asymmetrical with the degree of asymmetry depending on the point on the power frequency voltage wave at which the energization takes place and on the core residual flux. This potentially asymmetric flux waveform can have peak values which can easily saturate the core.

When a transformer core saturates, the impedance of the energized winding is greatly reduced because magnetic flux is forced out of the core and the impedance of the coil is decreased to, practically, its air core value. This causes high magnitude currents to flow in the winding whose peak values can exceed 10 times the transformer's rated current and persist for several seconds. Furthermore, the resulting current is asymmetrical leading to the presence of higher order harmonics. These energization currents are known as "Transformer Transient inrush currents", also commonly referred to as simply Inrush Currents (IC). The phenomenon manifests itself to both single-phase and to three-phase transformers.

1.2 Problem statement

For quite some time, it has been known that whenever a transformer is switched into service, high-magnitude transient currents lasting, in extreme cases, for several seconds can flow in the energized winding affecting adversely both the transformer integrity and the intended operation of protective devices. These transformer inrush currents are, for many decades, dealt with on the basis of mitigating their effects rather than preventing their generation. Their impact at the protective device coordination level, has traditionally been addressed by: a) Introducing intentional time-delays (often in the range of a few seconds) to desensitize the protective relays by the time these transient effects subside b) adjusting upwards the rating of primary transformer fuses to withstand the elevated inrush current magnitudes and ride through the inrush current transient. These practices however do not address the ever-present potential of these transient currents to cause mechanical damage to the transformer windings given that inrush currents could approach the magnitude of fault currents.

In terms of mitigating the magnitude of the transient inrush currents, several techniques have been proposed focusing on some form of controlled transformer energization schemes, namely: a) system supply voltage reduction, b) introduction of external controllers to mitigate the inrush current c) residual transformer core flux management and d) point-on-wave switching methods. Point on wave switching methods have received a lot of attention in recent decades due to the advent of more reliable switchgear and improved relay functionality.

The methodology selected for transformer inrush current reduction is determined by its cost and ease of implementation versus transformer size and customer impact assessment. A brief review of existing and recently proposed inrush current reduction methods, are provided in section 1.3. The main focus, however, of this thesis is to investigate switching methodologies for lower rating three-phase distribution transformers using breakers whose cost-range excludes individual pole control.

The method of using point-on-wave switching consists in energizing the transformer at an instant on the voltage wave, judiciously chosen to prevent the generation of high magnitude peak core fluxes, accounting for existing residual core fluxes. Suitable switching methodologies have been proposed in the past, for the determination of an optimal closing point for both type of the above-mentioned switching approaches resulting in either optimal or near-optimal switching.

1.3 Review of transformer inrush current mitigation approaches

Several transformer inrush current mitigation techniques have been proposed over the years each with its own advantages and disadvantages. Not all of them, however, are easily implementable or economically feasible. In what follows, the salient aspects of several of these proposals, are reviewed. Given, however, that this thesis centers on point-on-wave switching, these techniques are reviewed in more detail, in section 1.3.4.

1.3.1 Application of external resistors

The application of external resistors has been a time-honored technique to reduce the prospective transformer inrush current. One can distinguish between two kinds of resistor application technologies, namely:

a) **Insertion of external line resistors:** [1] i.e. resistors connected on-line for all three phases between the source and the transformer winding to be energized. These resistors are effective in mitigating core flux excursions, under virtually any core fluxing conditions, given that the voltage applied to the energized winding is less than the available supply voltage due to the ensuing resistance voltage drop, across them. These switching resistors are larger than the typical resistors one would use for line/cable switching transient current limitation purposes and must be kept in the circuit much longer, given that the duration of the inrush current could persist for several seconds Timing their insertion and removal is one of the issues that need to be addressed whenever they are employed. Equally important, related issues are the complexity and cost of the controls involved to incorporate them in the energization switchgear, given that voltage transients during resistor insertion/removal must be properly managed. The above considerations limit the application of the still popular line resistor insertion technology to rather larger station transformers.

b) **Insertion of neutral resistors:** These are grounding resistors and are connected at the neutral of the three-phase winding that will be energized [2]. This method is, less expensive compared to the line resistor scheme, given that only one resistor is used. As far as the residual flux calculation is concerned, a data acquisition system can record the discrete voltage waveform at the transformer terminals and residual flux calculation is initiated at voltage zero crossing [3]. For a three-core three-phase transformer, the phase exhibiting the highest residual flux is first energized. The inherent magnetic circuit interaction with the remaining two core legs generates the so called dynamic core fluxes upon energizing any phase, a situation that does not preclude inrush currents when the remaining phases are switched.

The scheme is most effective when one phase is switched first. Its effectiveness is reduced when the other phases are switched and overall performance considerations require tuning the neutral resistor value to entertain proper inrush current levels for all three phases. In case of simultaneous switching of all three phases an inrush current reduction of, at best, 20% can be expected [4, 5]. It is clear that this technique can be applied only to transformer energization from a Wye-connected winding.

1.3.2 Transformer design-related considerations

The following approaches entail modification of transformer design aspects either at the core or winding level that will exert a mitigating effect on the potential inrush currents. More specifically:

(a) Reducing the iron core magnetic permeability by inserting air gaps in the core magnetic circuit, an action that typically reduces the remnant flux level by virtue of the higher magnetic core reluctance [6]. Furthermore, the linearizing effect of the air gaps on the iron core characteristics, makes the transient core flux response much less dependent on the initial remnant flux [7].

(b) Modifying the primary and secondary winding geometrical dispositions, through a two-layered winding structure, essentially increasing the transformer leakage reactance, thus reducing the resulting inrush current [8, 9].

Despite the claimed prospective success in inrush current reduction of the above mentioned methods, one needs to be mindful that both core and winding design for power transformers are, usually, governed by far more pressing design specifications than inrush current reduction. Intervening at the core/leakage reactance determination design stages of a power transformer are fundamental design adjustments that may seriously affect the overall power transformer performance and its total resulting cost.

1.3.3 Residual core flux management

Given that the residual core flux serves as the initial condition to the flux excursion transient upon transformer energization [10], the following approaches have been suggested to manage its levels at the instant of energization: (a) Core demagnetization by constant-frequency variable-voltage external excitation whereby the winding flux is reduced by successive reduction of the externally applied DC voltage levels in every consecutive half cycle (b) Core demagnetization by variable-frequency, constant reverse voltage, which reduces the residual core flux amplitude by gradually decreasing the time interval of successive voltage reversals, i.e., increasing the frequency of voltage reversal. This is more effective than (a) as core residual flux reduction/elimination is obtained quickly and the physical realization is simpler [11]. (b) Pre-fluxing the transformer, i.e., force the core residual flux to assume a large magnitude of desired polarity [12]. It should be mentioned that the latter method does reduce the inrush current but cannot eliminate it.

The uncertainties on residual flux estimation are limited by performing energization and de-energization rapidly with a delay of 2 seconds. Synchronous dual trigger signals at zero crossing of line voltage are used to control the time of energization and de-energization. The residual flux is evaluated as the integral of winding induced voltage and once it reaches stable value its assumed constant until the next energization [13]. The authors of [14] propose a switching-on angle control determined by PC-AT microcomputer from which the signals are sent via D/A converter.

In general, residual core flux management techniques need additional apparatus to perform either core demagnetization or pre-fluxing [15] something that makes them dependent on supplementary apparatus. It should also be mentioned that the residual core flux magnitude is dependent on core material and load power factor. The exact levels of core residual flux cannot be established with certainty and can exhibit quite large variability. [16] Recent typical residual core flux calculations following typical energization performance studies for step up wind farm transformers [17, 18] yielded values between 0.4 and 0.8 pu.

1.3.4 Point-on-wave controlled switching

Ever since the early quantitative investigations of the single-phase transformer inrush current dynamics, it has been ascertained that in the absence of residual core magnetization, the most favorable switching moment is at the voltage supply crest instant, given that at this moment the prospective magnetic flux level is zero, thus minimizing the subsequent transient flux excursion and thus the peak value of the ensuing inrush current. On the contrary, energizing the transformer at voltage zero would cause much larger transient flux excursions. These realizations form the foundations of “point-on-wave switching”, i.e., properly timing the instant energization takes place vis a vis the voltage supply waveform temporal variation.

Inrush current minimization with residual core flux, be it for single or three-phase transformers, follows the same principle, given that residual flux levels and improperly timed voltage energization can conspire to produce excessive inrush currents. It is a well-known result that, in the presence of residual core flux, the most advantageous switching moment on the incoming voltage wave is the one that yields a prospective core flux equal to the residual flux [10].

Although the problem seems to have a well-defined answer for single-phase transformers, the situation is quite different for three-phase units given that: a) not only one but three-phase voltages produce, concurrently, magnetic fluxes and b) the magnetic circuitry of three-phase transformers could assume different geometrical construction, greatly affecting the eventual formation of residual and dynamic core flux patterns, upon disconnection/energization. It becomes therefore necessary to pay closer attention to transformer post-disconnection performance that critically shapes residual core flux levels in the presence of, among other factors, the ensuing sustained oscillations with either intentionally connected or parasitic winding capacitances.

Three switching strategies have been developed [19, 20] in order to eliminate inrush current in three-phase transformers, namely:

(a) **Rapid closing strategy** - This switching sequence closes one phase first and the remaining two phases within approximately one quarter cycle of the supply service frequency after that.

(b) **Simultaneous closing strategy** – This switching scheme closes all phases together at an optimal point that emulates the single-phase closing strategy under residual flux, i.e., the residual core flux patterns matches a prospective steady state flux pattern. Its application renders optimal performance however, only in very particular cases

(c) **Delayed closing strategy** – This switching sequence closes one phase first and the other two phases within 2-3 cycles of the supply service frequency after switching the first phase.

It is worth noting that both the Rapid and the Simultaneous closing approach require prior knowledge of the complete residual core profile, i.e. the residual flux must be known in all three windings This is not, however, the case for the Delayed closing strategy that requires the knowledge of the residual flux of one phase.

1.4 Contribution

This thesis proposes a point-on-wave switching strategy to minimize inrush currents in transformers switched by means of gang operated circuit breakers. It is based on extensive and exhaustive simulations of opening and closing times of the breakers under a large number of different operating conditions, namely associated with the time the breaker is opened and the resulting residual flux. From these simulations, closing instants that result in the lowest inrush current in any of the three-phases for any residual flux are tabulated and used to set the breaker point.

A supplementary closing angle determination time criterion is also proposed based on minimization of estimated and actual fluxes. This method confirms the results obtained using the brute force search approach.

1.5 Methodology

The proposed solution is investigated for: a) three-phase distribution transformers composed of either three single-phase units and/or three-phase frame-cores assemblies; b) different transformer core nonlinear characteristics; c) transformer core residual flux profile-dependency on the magnetic core geometrical disposition and d) transformer energization from either a Wye or a Delta winding.

The methodology consists in running simulations of transformer switching using the Matlab/Simulink software package. Transformer models available in that package were used and adapted to the specific cases. Actual field data were used to set the residual flux is entered in the transformer model for the different simulation runs. The inrush currents were obtained for the different test cases determined by typical field situations and operating conditions.

Several core constructions with their own residual core flux profiles, as obtained from field measurements, are considered and the ensuing inrush peak magnitudes are calculated for several typical winding connections.

From the inrush current information, the closing times corresponding to minimum inrush current are established. This thesis however does not address issues related to circuit breaker operation.

1.6 Thesis Summary

This thesis is organized as follows:

Chapter 2 reviews the fundamental mathematical framework of the inrush current phenomenon as manifested on single-phase transformers, its potential repercussions and the fundamental principle of the point-on-wave switching approach for inrush current reduction. It then extends the notions elaborated to three-phase transformer units and reviews the state of the art switching methodology.

Chapter 3 describes the simulation framework used in this thesis in terms of transformer core model geometrical configuration, magnetization characteristics and equivalent circuits.

Chapter 4 contains the actual simulation results using the brute force search approach in determining the optimal closing instant. A simplified closing rule of thumb is then deduced based on these simulation results. It is applied to various transformer winding and core configurations and its effectiveness is established. It is shown that the estimation of the closing times can be expressed mathematically as a minimization equation. Results obtained are similar to those of the brute force search.

Chapter 5 encapsulates the conclusion of this thesis by summarizing the point-on-wave switching strategies suggested for gang operated circuit breakers and their performance on effective reduction of inrush currents. The chapter concludes with the recommendations for further extension of the suggested switching technique.

Chapter 2 Transformer Inrush Transients and Switching Techniques

2.1 Introduction

This chapter reviews the analytical base of the inrush current development in single-phase transformers. Based on the mathematical model presented herein, the inrush current mitigation approaches already outlined in the previous chapter are put into proper perspective and the basic principle behind point-on-wave switching clearly emerges.

2.2 Single-phase transformer switching

The steady state magnetizing current of a transformer is, typically, 1-2 percent of the rated operating current but capable of becoming as high as 10-20 times that when switched, across the line. The fundamental equations [21] illustrating the phenomenon are as follows:

By Faraday's law,

$$v(t) = N(d\varphi/dt) \qquad (2.1)$$

Where,

$v(t)$ - induced voltage across the winding

$\varphi(t)$ - Flux through the winding

When the transformer is energized at a supply voltage minimum, i.e. at a voltage supply zero-crossing, and assuming, zero voltage drop across the supplying cables,

$$v(t) = V\ sin(\omega t)$$

Substituting and integrating for maximum flux in a half cycle,

$$\varphi(t) = \frac{1}{N}\int_0^{\pi/\omega} V\sin(\omega t)\,dt \qquad (2.2)$$

$$= -\frac{V}{N\omega}\cos(\omega t)\Big|_0^{\pi/\omega}$$

$$= -\frac{V}{N\omega}\ [(-1) - (1)]$$

Hence for zero residual core flux,

$$\varphi_{max} = 2(V/\omega N) \qquad (2.3)$$

It is seen that, under the circumstances, the maximum transient flux excursion is twice the steady state prospective flux. The transformer core will saturate, thereby yielding a magnetizing inrush current that can be of quite high magnitude.

When, however, the transformer is energized at a supply voltage maximum,

$$v(t) = V\ sin(\omega t + 90^0) \qquad (2.4)$$

We obtain that upon integrating for maximum flux in a half cycle,

$$\varphi(t) = \frac{1}{N}\int_0^{\pi/\omega} V\cos(\omega t)\, dt$$

$$= -\frac{V}{N\omega}\ \sin(\omega t)\Big|_0^{\pi/\omega}$$

$$= -\frac{V}{N\omega}\ [(0) - (1)]$$

Hence, again for zero residual core flux and no supply- related voltage drops, we obtain

$$\varphi_{max} = (V/\omega N) \qquad (2.5)$$

In this condition the maximum attained core flux is equal to the steady state crest prospective flux and the transformer does not enter into saturation, thus eliminating the undesirable inrush current.

Transient flux excursions can be even more severe if core residual flux is accounted for. In Figure 2.1, when the transformer is energized at point X (voltage maximum), the transient flux is the residual flux, now different from zero.

The applied voltage at time t_0,

$$v(t) = V\ sin(\omega(t + t_0)) \qquad (2.6)$$

Substituting and integrating,

$$\varphi(t) = -(V/\omega N)cos\big(\omega(t + t_0)\big) + c \qquad (2.7)$$

Substituting $(V/\omega N) = \varphi_{max}$ (peak normal flux) and at time t_0, $\varphi(t) = \varphi_R$ (residual flux), we obtain that:

$$c = \varphi_R + \varphi_{max}cos(\omega t_0)$$

The core flux, therefore, as a function of time can be expressed as

$$\varphi(t) = \varphi_R + \varphi_{max}cos(\omega t_0) - \varphi_{max}cos(\omega(t + t_0)) \qquad (2.8)$$

Solving for worst case peak flux one obtains,

$$\varphi_{peak} = \varphi_R + 2\varphi_{max} \qquad (2.9)$$

Solving for energizing at a supply voltage maximum (zero prospective flux) per Figure 2.1, we obtain

$$\varphi_{peak} = \varphi_R + \varphi_{max} \qquad (2.10)$$

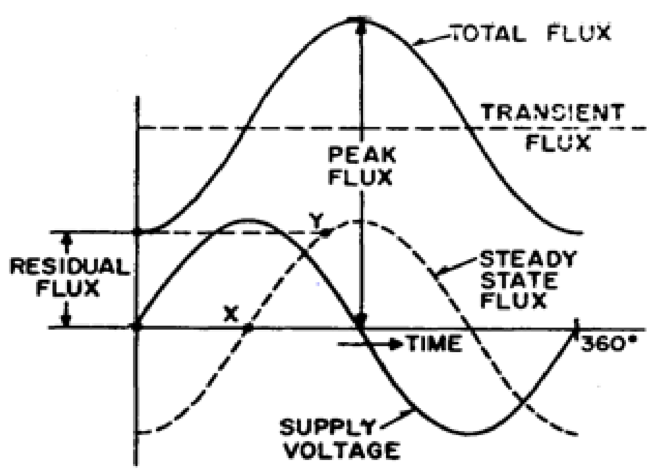

Figure 2.1 Transformer energization transient core flux variation patterns [10]

The optimal way in order to reduce the inrush current would be to energize when the residual flux is equal to the prospective flux i.e., at point Y as seen in Figure 2.1 applying power frequency voltage with the residual flux as the initial condition of the core flux at the instant of energization, will lead to a superimposition of applied flux at that instant with the residual flux, leading to asymmetry (since the flux is offset) in the core flux as shown in Figure 2.2

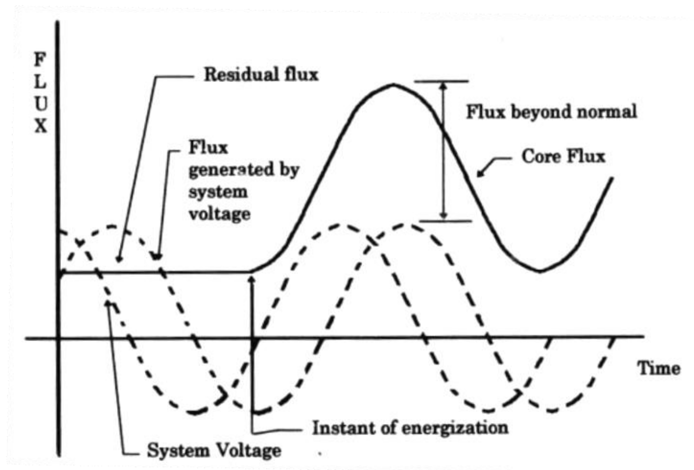

Figure 2.2 Core flux under worst-case energization for a given residual flux [10]

The following figures illustrate the energization of a single-phase unloaded transformer. Figure 2.3 shows the primary excitation current of the unloaded transformer. Figure 2.4 represents the excitation current of the same unloaded transformer with energization occuring at a voltage minimum. It is seen that, the transformer is pushed into saturation with the subsequent generation of highly asymmetrical harmonic-rich inrush currents. The magnetization characteristic of the core was taken to be a two-segment piecewise linear curve with the saturation core level at its knee.

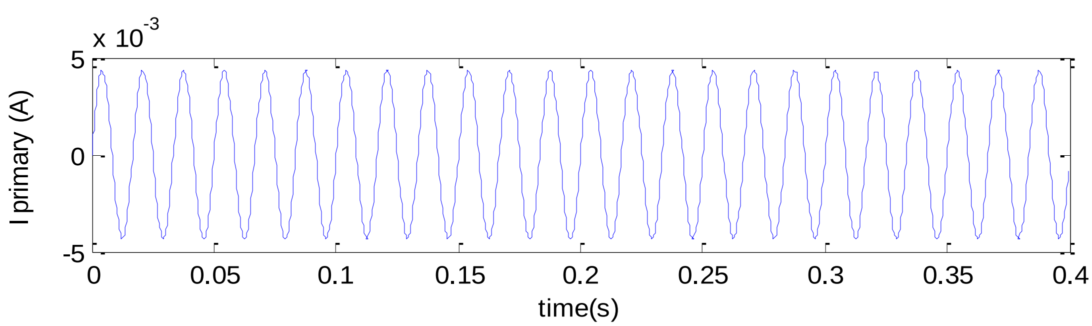

Figure 2.3 Unloaded transformer primary (magnetization) current

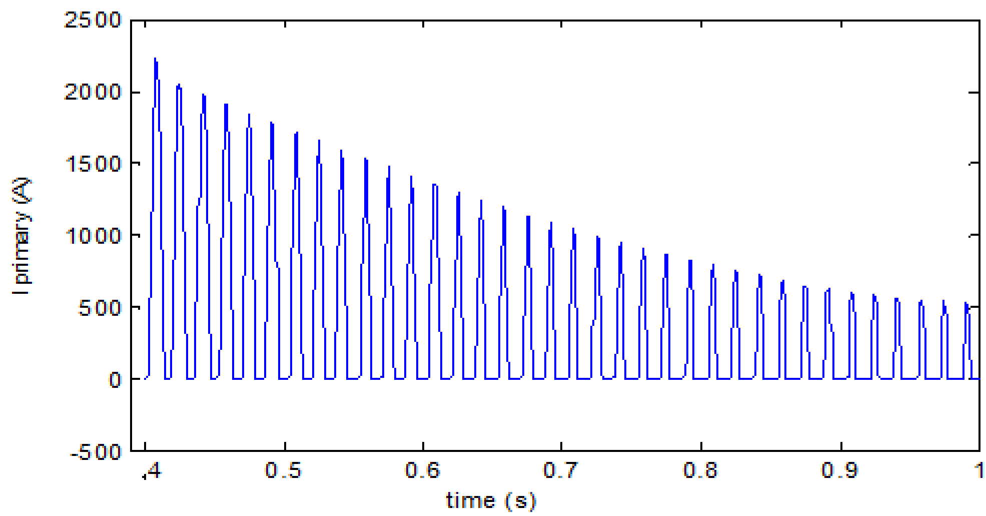

Figure 2.4 Transformer primary current after energization at 0.4 seconds

2.3 Inrush current characteristics

The analytical treatment above quantified the maximal core fluxes vis a vis the residual core flux and the moment of energization. Physically, the phenomenon manifests itself as significant amounts of flux being driven outside the saturated transformer core, making the magnetic core structure behaving, essentially, as an air core system. The resulting inrush current asymmetry and its associated unidirectional component (DC offset) could be of either polarity, depending on point-on-wave energization moment and/or residual core flux levels.

The transformer energization from the HV winding side has been common practice over the years [22] given that, typically, the HV winding has a higher leakage inductance, being wound concentrically around the LV winding at a larger mean radius. The magnetic non-linearity of the transformer core resulting in successive oscillations of effective impedance between air core and iron core characteristics is the very source of the inrush current harmonic content.

The duration of the inrush currents is based on source resistance and transformer losses [23] i.e., with high source resistance and losses more damping is introduced to the transient phenomenon and the inrush current duration is shortened. Based on these remarks it is not unusual for generating/substation transformers to anticipate quite severe and longer-lasting inrush current phenomenon.

2.4 Inrush current consequences

Inrush current magnitudes could, in extreme cases, approach the magnitudes of short circuit currents with adverse consequences on the supply power system, intended protection functionality, power quality and the integrity of the transformer itself. The main impact the inrush phenomenon could have on the power transformer is structural, due to the mechanical stress that could be exerted on the energized winding. Despite the fact, however, that the magnitude of the inrush may be less in magnitude than the prospective fault current, the resulting mechanical stresses have a cumulative effect due to the: a) potentially longer duration of the inrush phenomenon and b) frequent switching particularly at the distribution environment. Due to ensuing mechanical stress, the transformer may experience overdue mechanical winding displacements thereby leading to either direct mechanical or insulation damage, both being rather non-trivial to detect on an “a-priori” preventive maintenance basis [6]. Other, less equipment threatening but quite annoying, effects of inrush current typically include false operation of primary transformer fuses, sympathetic inrush in other already functioning near-by distribution transformers, transient over voltages and commutation failures of HVDC converters [24] all related to inrush current-induced compromised power quality.

2.5 Transformer disconnection and residual flux

When the transformer becomes disconnected from the supply grid, some magnetic flux remains within the core as a consequence of the well-known hysteresis property of the ferromagnetic. Given that transformer cores are usually made from “soft” ferromagnetic materials, residual flux core levels are not, in general, that significant. They are however sufficiently large to generate the inrush phenomenon.

A reduction of the residual core flux levels can, take place as a result of a natural energy oscillation resulting from the channeling of the stored magnetic energy in the core towards any real and/or parasitic winding-related capacitances. This energy oscillation is not lossless and results in a typically smaller value for the residual core flux, as compared to the residual flux an ideal lossless interruption would have yielded. The phenomenon is also known as the “ring-down” transient.

The ring-down phenomenon can be modeled in some detail, assuming proper data availability. In some cases, it is of significance whenever conditioned transformer disconnection to yield proper residual flux patterns is sought.

No ring-down transients are modeled in this thesis, given that the focus is not on managing transformer disconnection procedures. Instead, what is of interest here is determining optimal/near-optimal switching conditions for distribution transformers assuming a rather random residual flux profile.

2.6 Three-phase transformers and inrush current development

The transient inrush phenomena, described in section 2.2 for single-phase transformers, manifest themselves equally well in the case of three-phase transformers. In fact, the three-phase transformer lends itself to additional investigation, given that:

a) The three-phase transformer cores may assume several geometrical constructions ranging from three single-cores, (one for every phase), to three-legged, four-legged and even five-legged cores for special units meeting particular design specifications and/or auxiliary windings. The direct relevance of the core geometrical construction to the development of the inrush current phenomenon is apparent given that residual core flux levels for all phases are directly dependent on the reluctance of the core limbs and their connecting yokes.

b) The electrical connection of the three-phase transformer windings bears a great influence towards determining not only the prospective but, also, the actual core fluxes at the time of energization of any remaining phases. Last but not least, ring-down effects are also present in three-phase units. Again, they will not be of concern here for three-phase transformer closing transients.

2.7 Three-phase transformer switching strategies

This section reviews the salient aspects of three switching strategies currently used to eliminate/minimize the inrush current during three-phase transformer energization [10]. Depending on the core geometrical configuration and/or winding connections they can either eliminate the inrush current resulting in optimal switching or significantly reduce it

All the discussed techniques rest on point-on-wave switching principles in the sense that the moment of energization is determined on the phase(s) voltage wave, for one or more phases. They also depend on the knowledge of the core flux profile (for one or all phases) at the moment of energization, in order to ensure an inrush current that it will be as least as possible according to switching criteria already mentioned. An important notion in properly comprehending the underlying philosophy of three-phase transformer switching strategies is the notion of "dynamic flux". The term dynamic flux refers to the value(s) the magnetic fluxes the transformer core legs of all three phases experience over time, factoring-in the effects of residual core fluxes, once any phase(s) is first switched-on to the voltage supply source. Dynamic core leg fluxes will determine the inrush current levels at the moment of switching of the remaining phases, given that they act as initial conditions at the very moment(s) of their switching.

The techniques, whose description follows, are most effective for three-phase transformers that satisfy the condition of flux-dependency in terms of dynamic fluxes, i.e. the dynamic fluxes for the phase core legs sum up to zero.

2.7.1 Rapid closing strategy

This strategy closes one phase first and the remaining two phases simultaneously after a time delay. Typically, all 3 phases will be eventually closed within a maximum pole time span of slightly over ¼ cycle of the service frequency.

Under zero residual flux conditions, the dynamic fluxes are evenly divided in the non-energized phases and the optimal energization point for the remaining two phases is 4.17ms, which is 1/4 of the service frequency cycle for a 60 Hz system, after first phase energization.

If the residual core flux pattern assumes the typically reported in the literature pattern of $[0, \varphi_R, -\varphi_R]$, the phase with zero residual flux is typically selected to be switched first and a delay of approximately 0.7 ms, for a 60 Hz service frequency, needs to be introduced to achieve optimal closure of the other two phases[10].

For non-zero residual flux conditions a modified closing time, other than the ¼ cycle, needs to be introduced for optimal closing conditions. The first phase, however, must still be energized in a transient free mode as already explained. It can be proved that, under flux-dependency conditions, and once the first phase is energized in a transient free manner, the remaining two phases will also achieve optimal closing conditions, in that their prospective fluxes will equal the dynamic fluxes, within approximately 2.4 to 4.17 ms or 4.177 to 4.24 ms, if the flux patterns differs from the symmetrical one mentioned above. These switching times are figures of merit and they pertain to results obtained for specific transformers but they are typical for this sort of switching sequence. The variability of the closing times of the remaining two phases, due to the above mentioned conditions, can assume at the implementation level the form of a look up table that yields the optimal closing time of the remaining two phases using as time reference the closing of the first phase.

Transformer de-energization dynamics could also be factored in, if deemed necessary, but the essential constraint of this closing method is that knowledge about the residual core fluxes of all phases is necessary as well as the breaker hardware ability to reliably support independent pole closing.

The implementation of this strategy involves three steps, including two switching steps, namely:

1. The residual flux of each phase is determined.
2. The phase to be closed first is selected based on zero prospective flux timing
3. The remaining two phases will be subsequently switched based on appropriate timing as imposed by the residual flux profile.

2.7.1.1 Effects of Prestrike and Mechanical Scattering

The above described switching strategy assumes perfect timing in closing the breaker as well as no prior energization due to pre-strike effects. Given that the circuit breaker is a mechanical device that, by necessity, involves mechanical tolerances in its operation, the assumption of perfect timing in closing any pole phase is not realistic and mechanical scattering has to be considered along with its implications. Modern switchgear has reduced mechanical scattering by almost 50%, i.e. down to 1ms as compared to the typically cited 2 ms-2.5 ms cited in the literature a few decades back. The effect of mechanical scattering on properly closing the phase with zero residual is to close at a non-zero flux instant something that may not only cause inrush in that phase but may, also, result in a full cycle delay prior to establishing optimal closing conditions for the remaining two phases.

The prestrike effect is due to the fact that the approaching circuit breaker contacts may bridge their rapidly diminishing gap prematurely, around crest voltage yielding another source of error for the optimal flux closing condition. Adjustments based on the prospective flux slope can be provided using a look up table developed from suitable considerations.

The above mentioned situations manifest themselves also when energizing from a delta winding. More specifically: a) in a delta connected winding the division of flux in the remaining legs of a three-legged core is dependent upon the level of saturation and the leakage impedance of the winding and b) when energizing a delta-connected winding two phases must be energized simultaneously. Given that energizing one phase of the Delta, one supply voltage has a positive slope and the other a negative one the voltage stress across the pole contacts that close last is more severe leading to increased prestrike likelihood.

2.7.2 Delayed closing strategy

In this strategy, a delay of approximately 2 cycles is introduced for closing the remaining two phases, after the closure of the first phase.

This strategy affects only the last two phases to be energized and presents an advantage over the rapid closing strategy, in that there is a need to determine the phase with the smallest residual flux that needs to be closed first Instead, the determination of the residual flux of any phase will suffice rendering the technique easier to implement. The reason for this performance is the so-called “core-flux equalization” phenomenon. The strategy can be rendered even simpler if it so happens that the transformer core residual flux pattern follows the typical pattern $(0, \varphi_R, -\varphi_R)$ since in that case the phase with residual flux equal to zero can, conveniently, be the phase that is switched first [10].

The implementation of this strategy involves, again three steps, including two switching steps. The steps used for implementation are as follows:

1) Residual flux measurement on one phase

2) Close the selected phase at the optimal instant given by Eq.2.11 in order to ensure transient free switching conditions given that the closed phase may have a residual flux.

$$t_{op} = \left(\arccos\left(-\frac{\varphi_R}{\varphi_{max}}\right)\right)/\omega \qquad (2.11)$$

3) Close the last two phases simultaneously, approximately 2 cycles later, at a zero cross over voltage of the already switched phase.

This strategy can be applied to any flux-dependent transformer. The literature recommends closure of the last two phases 2 ¼ cycles upon closure of the first phase as a simplification [10]. It was also observed that at low flux levels, flux did not divide evenly in the delta connection which resulted in an over voltage.

2.7.2.1 Effects of Prestrike and Mechanical time Scattering

The closing time error in the first phase energization, as discussed earlier, will invalidate the effectiveness of simultaneous closing of the last two phases, given that their closing point occurs at different times. That is why it is still necessary to perform timing adjustments for the first phase closure time determination due to breaker prestrike and mechanical scatter considerations. It is also recommended to close the first phase on the increasing portion of the prospective flux wave given that, by the very nature of the prospective flux wave, there are two possible instants where the prospective flux matches the residual flux It is reported [10] that this strategy can reduce the peak inrush current by 97% while the reduction only amounts to 85-93% when breaker scatter time of 1 ms is accounted for. Nowadays, the improved breaker manufacturing has reduced the mechanical time scattering to even lesser delay. The 2-cycle delay introduced before closing the last two phases of the transformer is, typically, the time taken by the dynamic core flux equalization phenomenon to eliminate the effect of the original residual flux imbalance.

2.7.3 Three-phase closing strategy

This strategy eliminates the transient inrush phenomenon only under the conditions of zero residual flux in one phase and equal positive and negative residual flux are present in other two phases, and then under specific conditions. The main advantage of this method is that it does not rely on independent pole control closing mechanisms something that reduces the cost of the breaker, a situation typical for distribution breakers. It has been well known that the effectiveness of this closing technique depends on the deviation of the residual core flux from the optimally required closing conditions. Assuming typical residual flux patterns the technique can be quite effective even under significant core fluxing conditions, as is the case for the typically reported residual core flux pattern of (0,-70%, +70%) [10].

Chapter 3 Transformer Models

3.1 Introduction

Different transformer models are used for inrush current calculations such as a permeance network model or a 2D finite element model [25], Norton equivalent circuit model [26], coupled electromagnetic model [27], wavelet models [28-30]. This chapter deals with briefing the transformer models [31, 32] used in the simulations. There are two types of transformers discussed, a) Three-phase transformer with three independent cores b) Three-phase transformer with three-legged core. The transformer model specifications, magnetic characteristics and the equivalent circuits are detailed.

3.2 Iron core magnetizing characteristics

The transformer operation principle rests on the effective linkage of magnetic flux between windings through a ferromagnetic core which provides a low reluctance flux path. The absence of a core leads to rather poor flux linkage. The saturation level of the magnetic core is defined as the maximum value of flux below which magnetic linearity is preserved. Physically, the core flux is kept confined within the core, a condition that is violated under saturation conditions that can be caused by high-magnitude asymmetrical magnetizing currents due to random switching. Figure 3.1 and Figure 3.2 illustrates typical results for a three-phase transformer 2.25MVA, 25kV/575V, Delta-Y_g gang energized from the Delta winding.

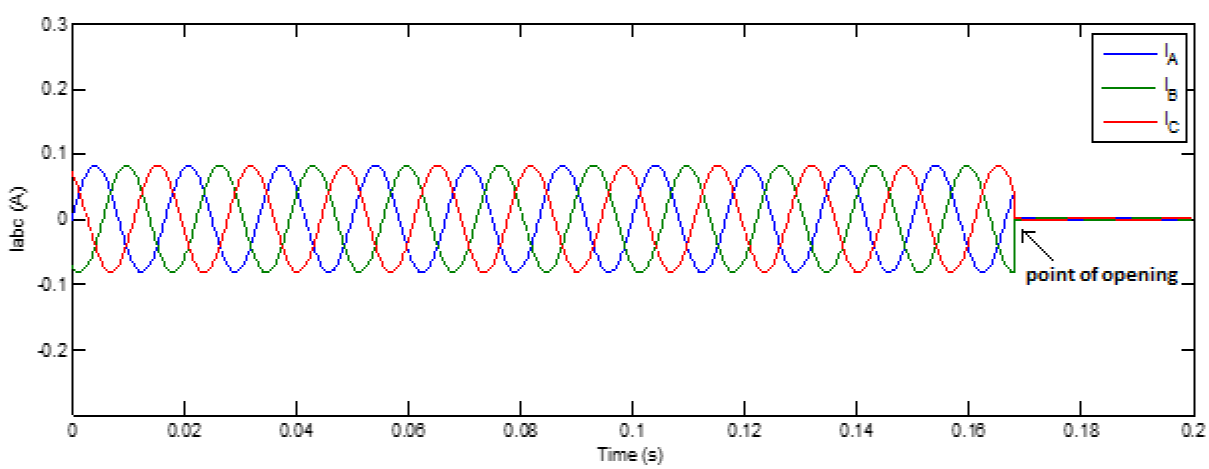

Figure 3.1 Line to line current waveform before breaker operation

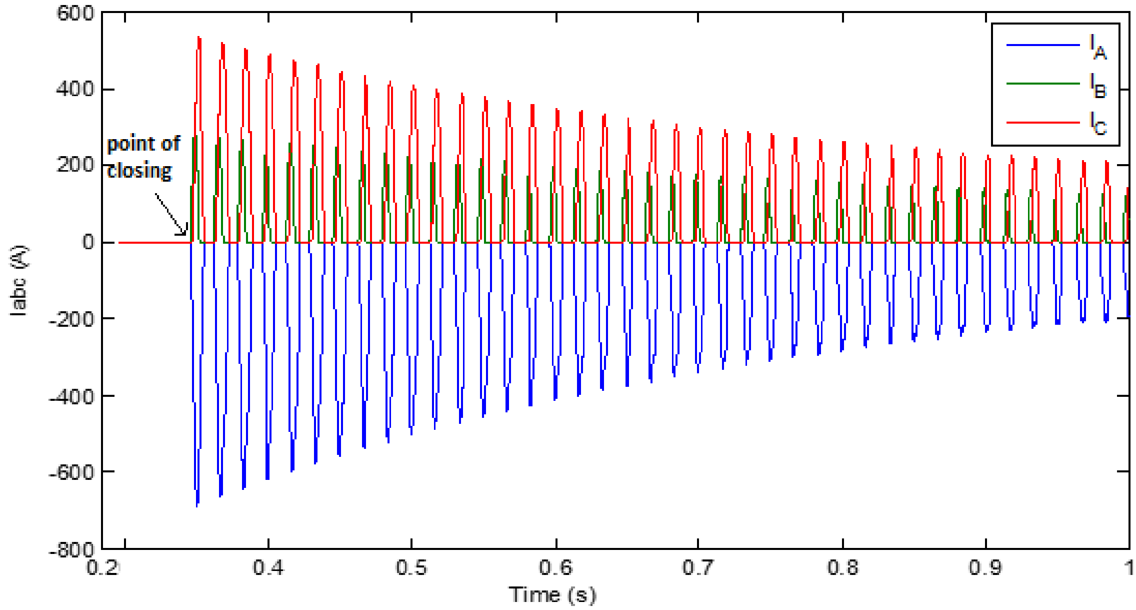

Figure 3.2 Line to line current waveform after energization

3.3 Three-phase transformer with three independent cores

This model implements a three-phase transformer using three single-phase saturable transformers. The transformer parameters and the saturation characteristic of the transformer are obtained from the EMTP-RV model [33] which are shown in Table 3.2 and Figure 3.4. For MATLAB implementation purpose, the three-phase saturable transformer model available in Simulink SimPowerSystems library was used. The magnetic core saturation model uses a piece-wise function with a second point near null excitation current to ascertain the slope of the non-saturated part of the magnetization characteristic [31, 34].

The transformer electric circuit is given in Figure 3.3, the parameters used in the transformer are shown in Table 3.1 and the non-linear inductance, Lsat is modeled using piecewise linear relationship curve which is illustrated in Table 3.2 and graphically represented in Figure 3.4.

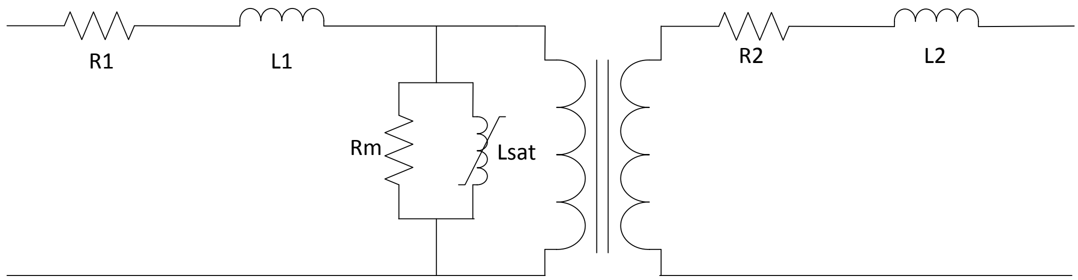

Figure 3.3 Transformer electric circuit

Table 3.1 Independent core transformer parameters

Nominal Power and frequency	Sn = 2.25 MVA, fn = 60Hz		
Primary Winding parameters	V1 = 25kV	R1 = 0.003 pu	L1 = 0.047 pu
Secondary Winding parameters	V2 = 575 V	R2 = 0.003 pu	L2 = 0.047 pu
Core loss resistance	Rm = 894.64 pu		

Table 3.2 Independent core magnetization characteristics

Current(A)	Flux(V.s)
0	0
0.000001	71.7069
0.140296	83.83126
0.187061	88.33459
0.280592	92.83792
0.467654	96.99485
0.654715	99.07331
0.935307	100.8054
1.434138	103.2302
1.901792	104.6159
2.883865	106.3479
4.894776	108.946
6.87451	110.1584
9.49337	111.7173
14.07638	113.2761
19.61028	114.1421
29.29071	115.5278
48.23069	117.2598
67.26419	118.4723
94.27899	120.3775
141.0599	123.322
187.7786	126.2665
280.7481	131.9823

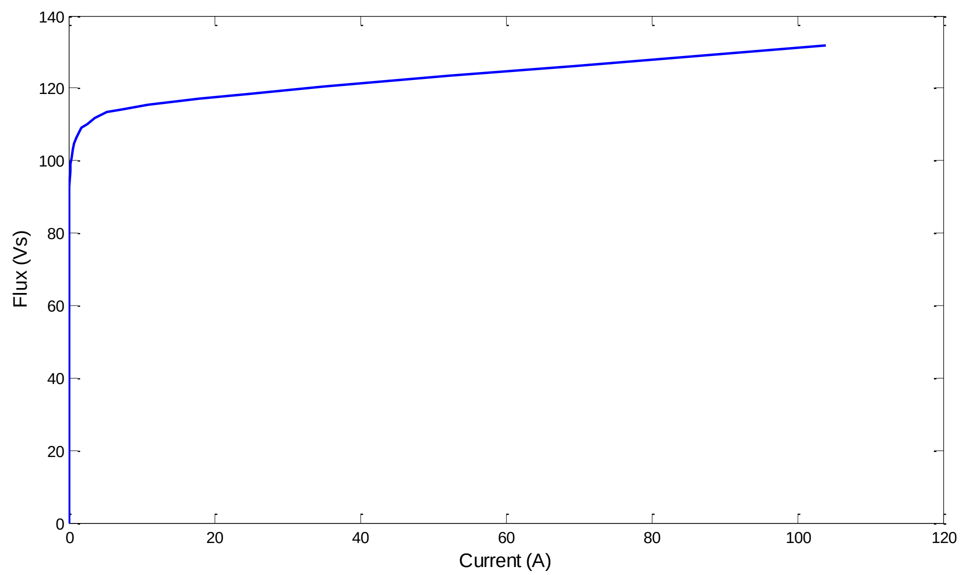

Figure 3.4 Core magnetization curve as per **Table 3.2**

3.3.1 Magnetic characteristics

The magnetic characteristics of this type of transformer is analyzed by a MATLAB/Simulink simulation. The absence of magnetic inter-phase coupling in this three-phase transformer model can be verified by energizing one phase of the three-phase assembly described above with a winding connection of Y_g-Y_g (Figure 3.5). It is seen that flux appears only in the energized phase (Figure 3.6) which verifies the absence of inter-phase magnetic coupling.

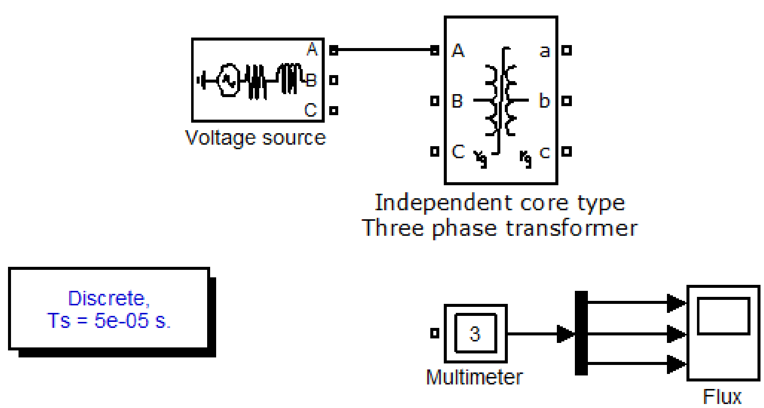

Figure 3.5 Single-phase energization of the three-phase independent magnetic core transformer

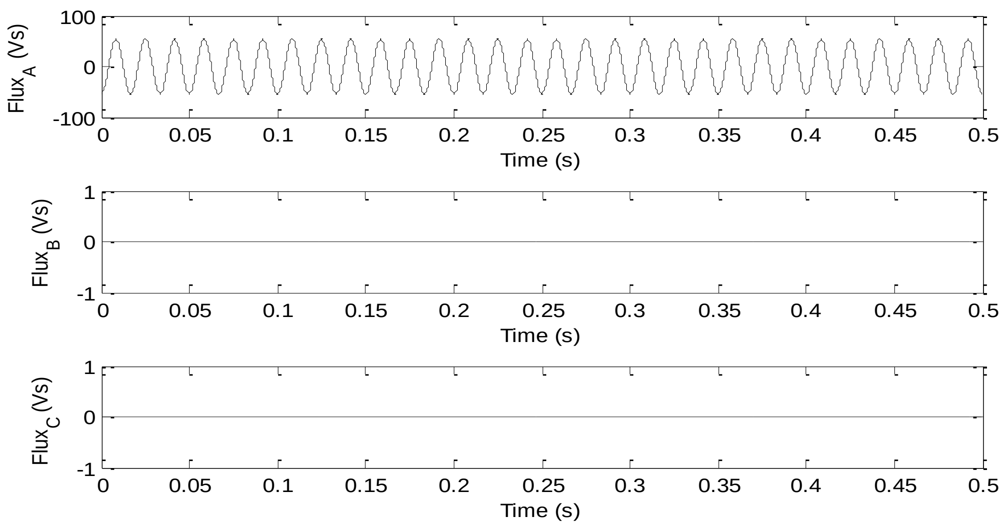

Figure 3.6 Flux waveform resulting from single-phase energization of three-phase independent magnetic core transformer

3.4 Three-legged core type transformer

A three legged core type transformer model [31] used in the simulations is described in the following section. The transformer design specifications and magnetic characteristics, transformer parameters are given in Table 3.3 and Table 3.4 respectively. The core structure of the transformer is illustrated in Figure 3.7.

Table 3.3 Three-phase Core type transformer design specifications and magnetic characteristics

BH Characteristics		**Design Specifications**	
H (A/m)	**B (T)**	Average Length and section of core limbs	L(m) = 53*2.54e-2
			A(m^2) = 45.48*2.54e-2^2
1/0.0254	0.45	Average length and section of yokes	L(m) = 21*2.54e-2
5/0.0254	1.2		A(m^2) = 45.48*2.54e-2^2
9/0.0254	1.4	Average length and section of air path for zero sequence flux return	L(m) = 0.5*2.54e-2
12/0.0254	1.47		A(m^2) = 45.48*2.54e-2^2
30/0.0254	1.51	Active power losses in iron (W)	225e3 * 0.02

Table 3.4 Three-legged core type transformer parameters

Nominal Power and frequency	Sn = 225 kVA, fn = 60Hz		
Primary Winding parameters	V1 = 2400 V	R1 = 0.01 pu	X1 = 0.05 pu
Secondary Winding parameters	V2 = 600 V	R2 = 0.01 pu	X2 = 0.05 pu

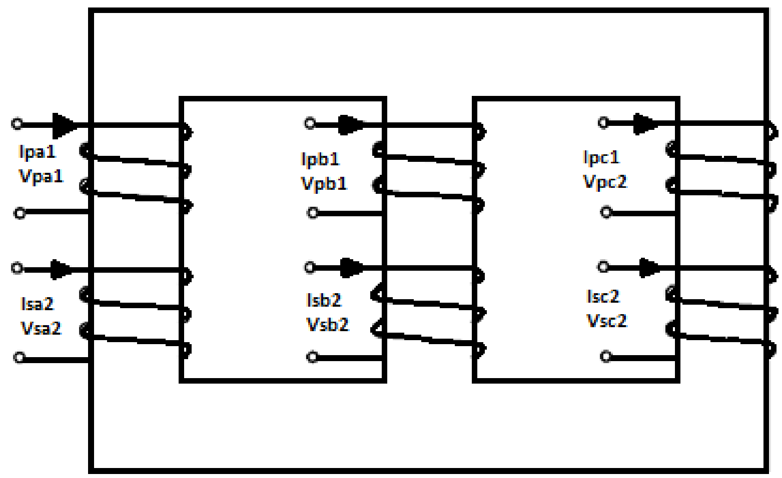

Figure 3.7 Three-legged Transformer Core Structure

The subscript "p" & "s" in the above figure represent the primary and secondary windings of the transformer respectively. The magnetic core equivalent circuit is given in Figure 3.8.

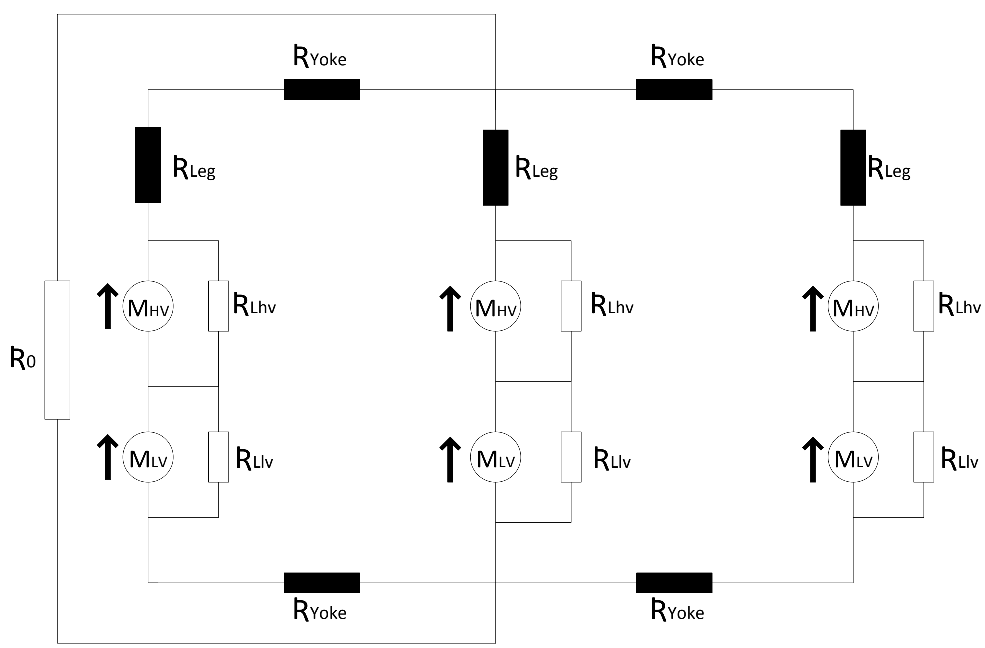

Figure 3.8 Equivalent magnetic circuit of three-legged core type transformer

Using Equation 3.1, the linear reluctances of the iron core limbs ($Ɽ_{Leg}$), yoke ($Ɽ_{Yoke}$) and leakage reluctances ($Ɽ_{Llv}, Ɽ_{Lhv}, Ɽ_0$) the values of which are given in Table 3.5 are evaluated from the B-H curve and the dimensions provided in Table 3.3. As we know the formula used for calculating the values,

$$Ɽ = \frac{l}{\mu A} \qquad (3.1)$$

Where,

l – Length of the circuit (m)

A- Cross sectional area of circuit (m[2])

μ – Permeability of material (H/m)

Table 3.5 Reluctance values for three legged core type transformer

Reluctance of core limb, $Ɽ_{Leg}$	212.16 At/Wb
Reluctance of yoke, $Ɽ_{Yoke}$	84.066 At/Wb
Leakage reluctance of windings, ($Ɽ_{Lhv}, Ɽ_{Llv}$)	803.83 kAt/Wb
Air gap reluctance of flux return path, $Ɽ_0$	7573.69 At/Wb

3.4.1 Magnetic characteristics

Fundamental excitation characteristics for a three-phase transformer using a three-legged core are shown in this section. The presence of inter-phase magnetic coupling following the single-phase energization procedure can clearly be seen in Figure 3.10, despite the absence of electrical coupling at the winding connection level, given that the latter is of Y_g-Y_g configuration.

In order to maintain the simulation consistency, the actual transformer parameters and the magnetic characteristics pertaining to the original model [31] is used instead of the transformer characteristics of the independent core transformer model.

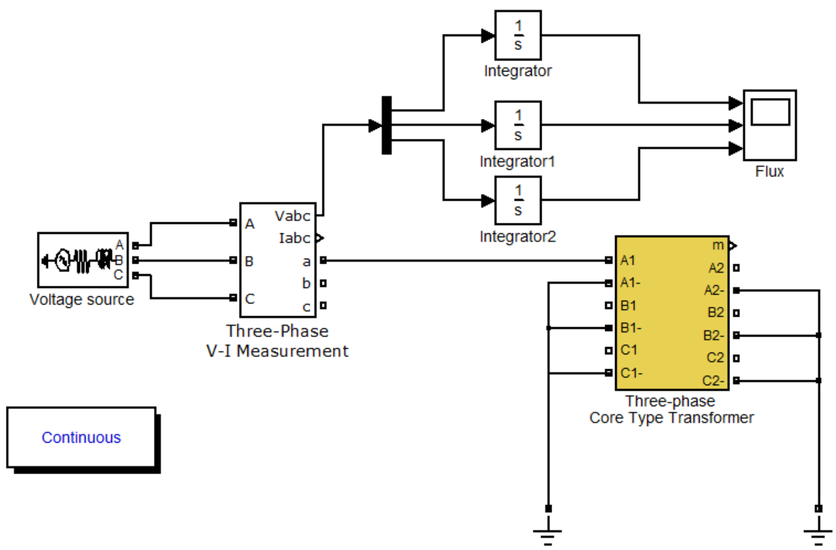

Figure 3.9 Three-legged core type transformer validation

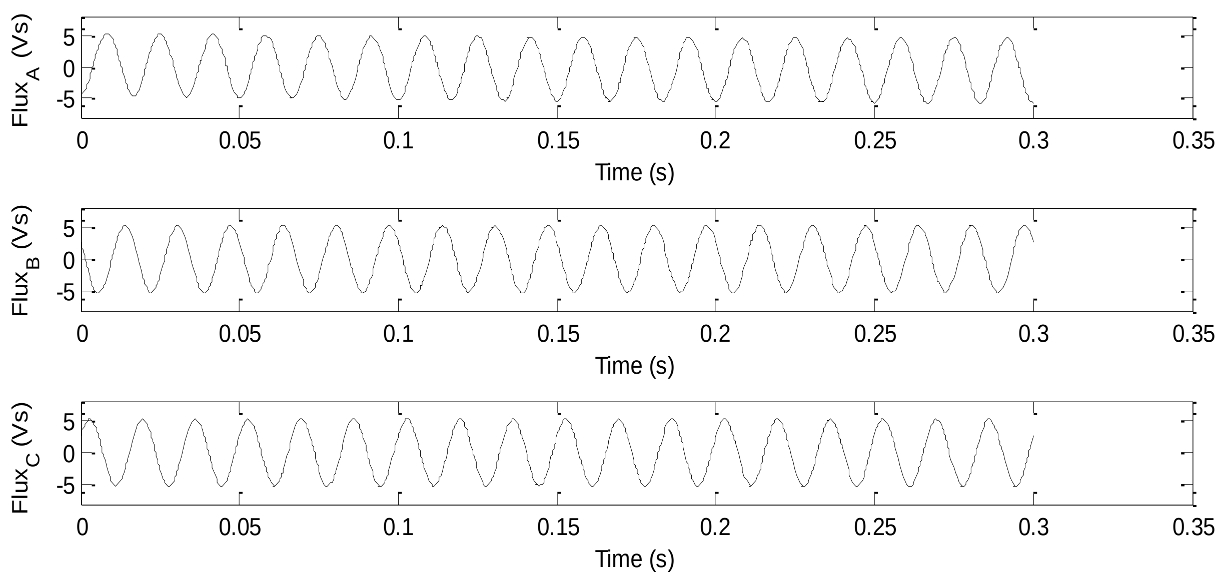

Figure 3.10 Flux waveforms for three-legged core three-phase transformer

The Simulink simulation setup used for simulating gang operation in three-phase transformer with independent core configuration is illustrated in Figure 3.11. A similar setup was used for the testing point-on-wave switching on the three-legged core type transformer with corresponding source and transformer parameters. The following chapter discusses the point-on-wave switching results obtained using this simulation setup in detail.

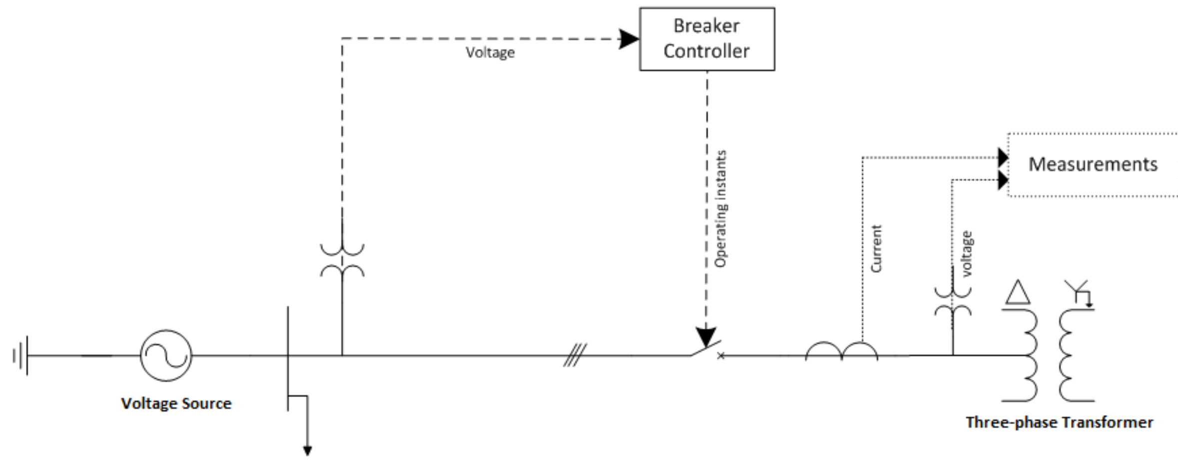

Figure 3.11 Simulation Model Arrangement

Chapter 4 Simulation Results

4.1 Introduction

This chapter contains the simulation results pertinent to gang-operated circuit breaker three-phase transformer energization. Results are provided for on different winding connections and for two different transformer models, one being a three-phase transformer consisting of three independent core structures and the other being a three-phase transformer with three-legged core structure. Pertinent residual flux data used herein are actual field data given in the Appendix A.1.

4.2 Gang-switched transformer effect of opening and closing angles

This section illustrates the fundamental switching operations on a three-phase Delta-Y-grounded transformer composed of three single-phase units each with its own magnetic core. The plots in Figure 4.1 to Figure 4.4 show the results obtained from switching all three-phases simultaneously (gang-operation). The transformer bank is switched from the Delta side at random opening and closing angles and the results are analyzed.

In the simulation, the breakers are considered to be ideal in the sense that neither mechanical nor dielectric scattering is considered and all exciting currents are interrupted at their normal current zeros. In what follows, a sample opening and closing angle combination is considered and the plots of voltage, flux and generated inrush current in all 3 phases are shown for illustration purposes. The case depicted below corresponds to a random closing angle, thus generating visible inrush current in all three phases. The commands given to the model are detailed in Appendix A.2. These results, obtained in the MATLAB simulating environment are similar to results obtained from EMTP-RV.

Figure 4.1 illustrates the line-to-line voltages on the Delta side of the transformer bank when opening and closing at 60 degrees and 90 degrees respectively of voltage angle of phase A. The moment of interruption is the same for all three-phases as we are gang switching the transformer. Figure 4.2 illustrates the core fluxes prior to de-energization as well as the transient flux after energization. The value of the core flux at the moment of interruption is determined by the saturation curve. Figure 4.3 and Figure 4.4 show the no-load prospective magnetization currents and the post energization inrush line currents respectively.

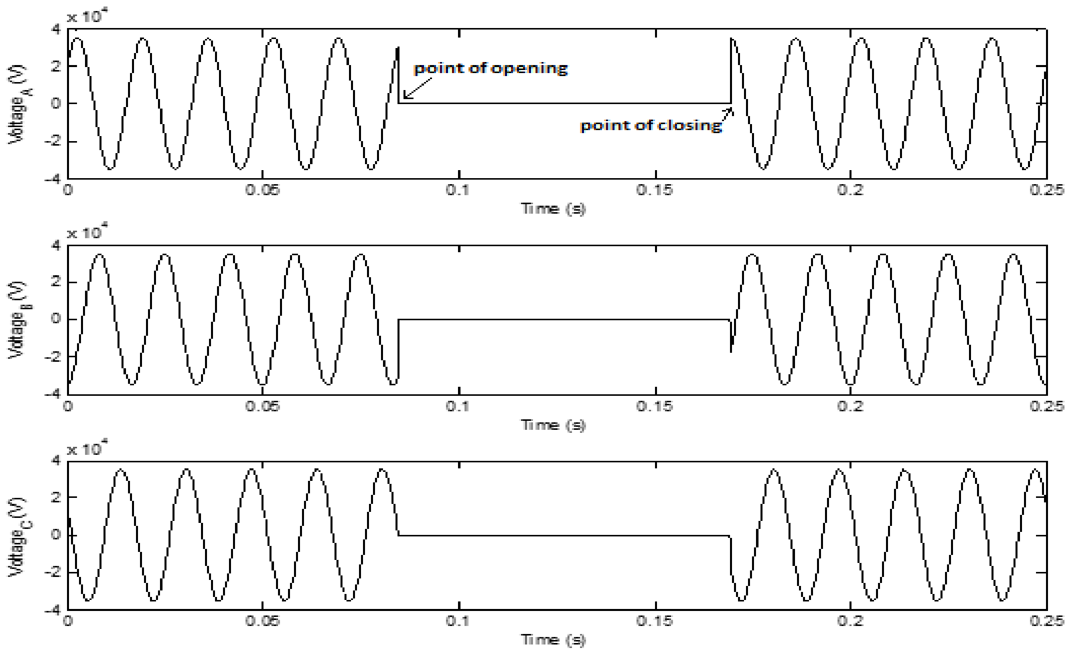

Figure 4.1 Line to Line voltage waveform (Delta side)

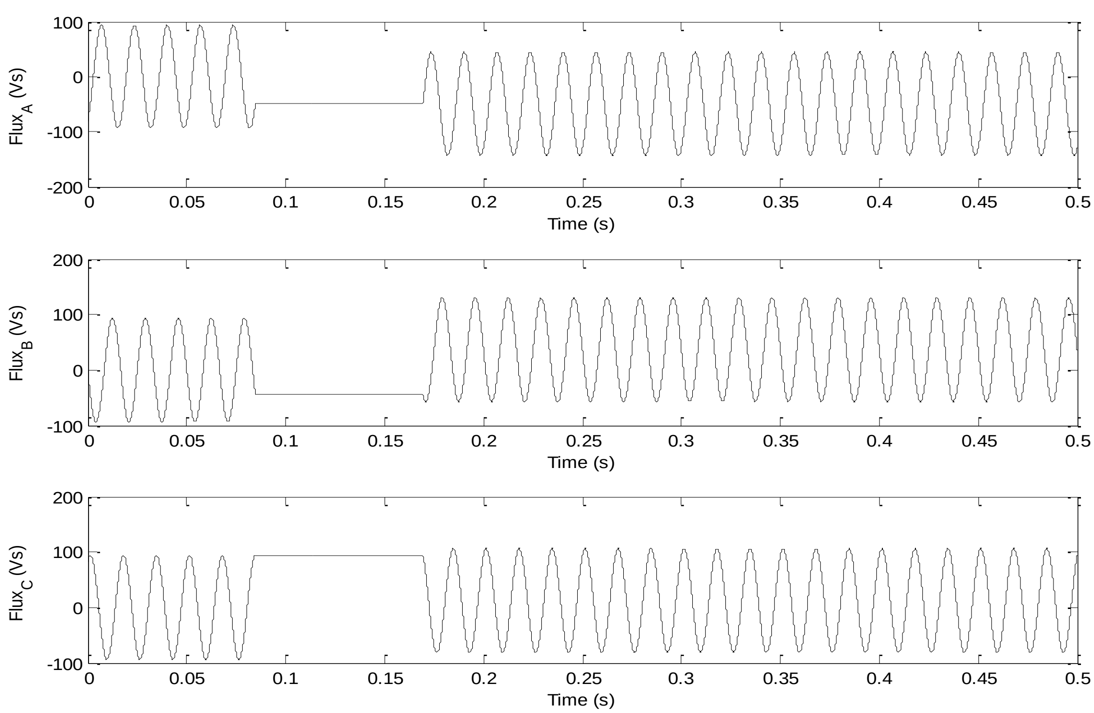

Figure 4.2 Flux waveform (Delta side)

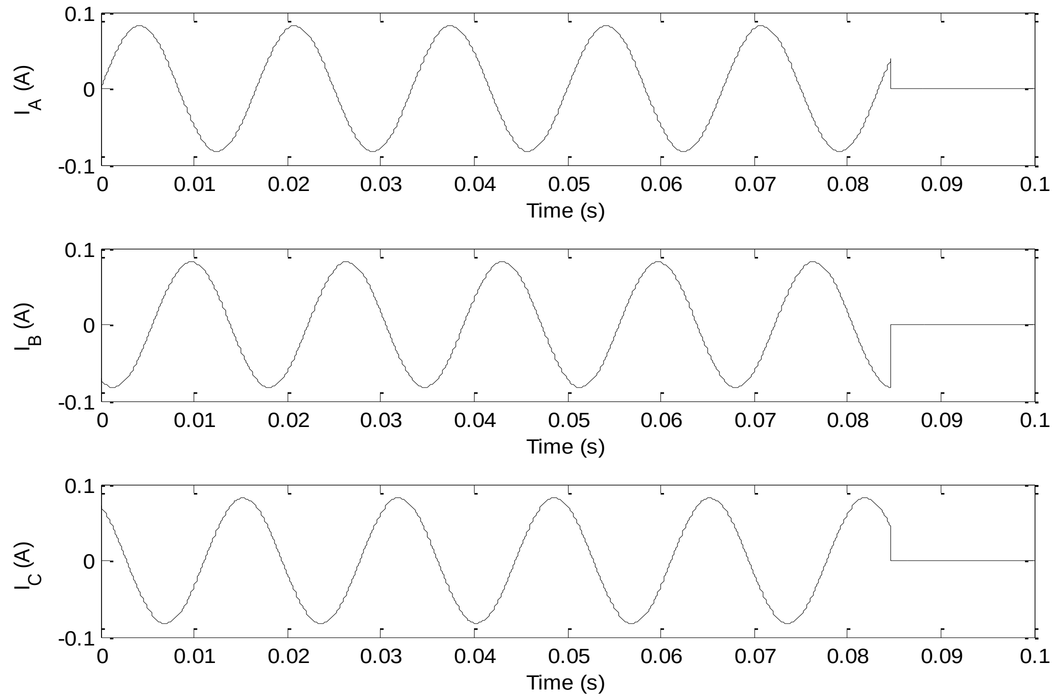

Figure 4.3 Line Current waveform before opening

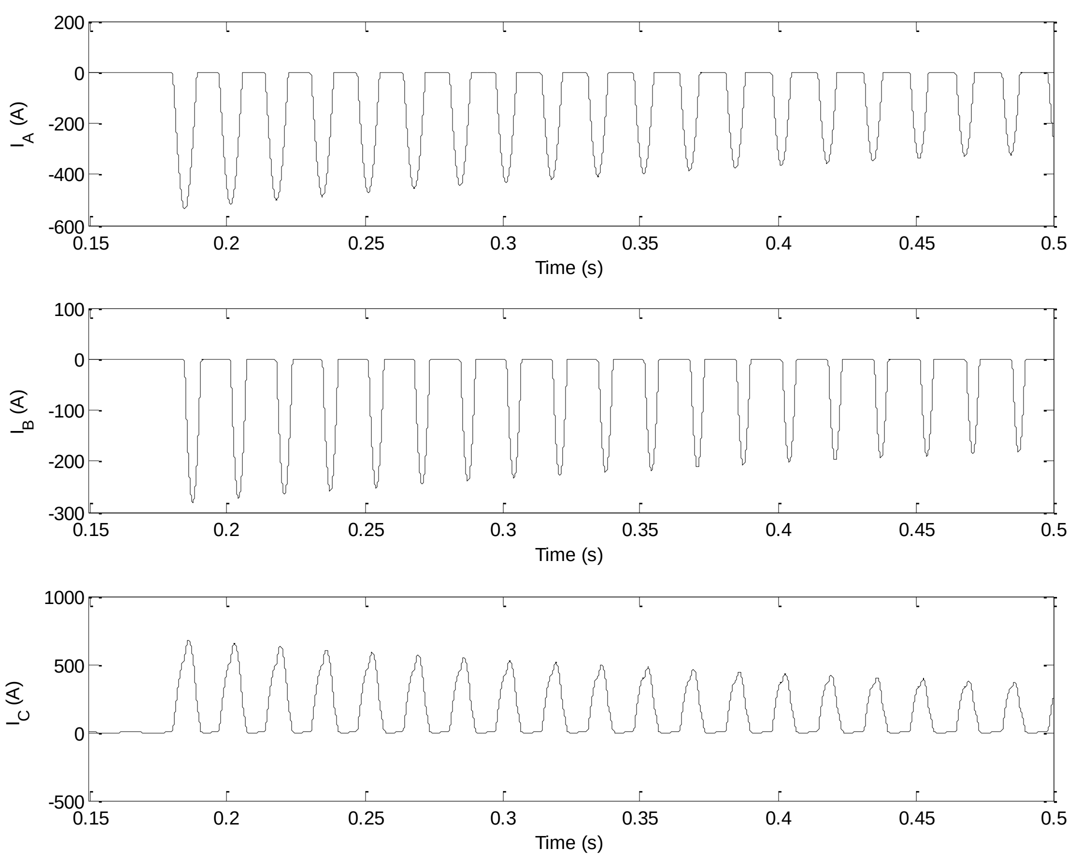

Figure 4.4 Line Current waveform after closing

From the results it can be seen that there is residual flux maintained by the transformer during de-energization and the phenomena of inrush currents are clearly noted when the transformer is energized again at random.

4.3 Gang-switching for various core saturation characteristics

Gang energization of a three-phase transformer (Delta-Yg) with independent cores [31] was simulated for different core saturation characteristics and the optimum closing angle assuming different opening angles was analyzed. The three saturation characteristics considered are listed below in both tabular (Table 4.1, Table 4.3 and Table 4.5) and graphical form (Figure 4.5, Figure 4.9, and Figure 4.13). The magnitudes of inrush currents reach as high as 35 pu in some cases due to the specific saturation curves assumed, as it is one of the factors affecting the inrush current magnitude. Residual flux levels are determined solely by the very opening angle. Figure 4.6, Figure 4.10 and Figure 4.14 portray the inrush current obtained as a function of the difference between opening and closing angles for all three considered saturation curves, while indicate some of the typical results used to construct them.

Curve 1:

Table 4.1 Saturation Characteristics curve 1

Current (A)	Flux (Vs)
0	0
0.000001	71.706
1	83.832
2	88.334
5	94.838
7	96.99
12	100.072
16	100.81
21	101
33	102.32
45	102.46
50	102.54
55	102.76

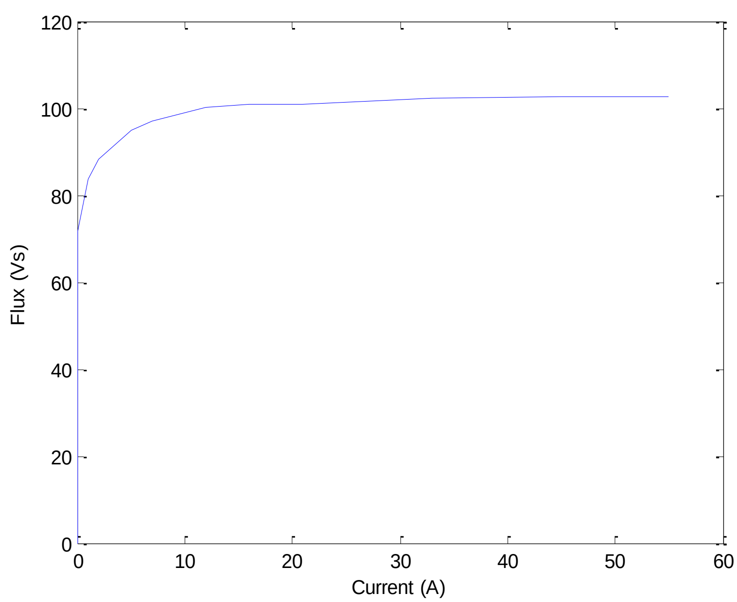

Figure 4.5 Saturation Curve for curve 1

Table 4.2 Opening at 270 degrees

Opening at 270 degrees	
Closing angle (deg)	Peak Inrush (pu)
0	23.65
30	26.73
60	33.6
90	37.02
120	33.83
150	25.57
180	22.6
210	13.35
240	4.10
270	0.04
300	4.72
330	14.18

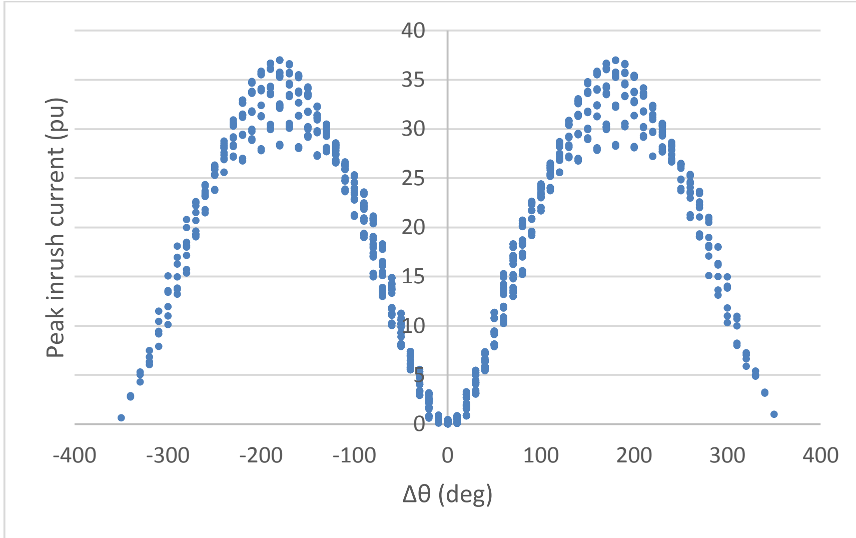

Figure 4.6 Δθ vs Peak inrush current

Table 4.2 shows that closing at the same opening angle of 270 degree results in the least inrush current amounting to 0.04 pu. Also shows that for Δθ equal to zero, the value of inrush current is the least. Figure 4.7 and Figure 4.8 illustrate the peak inrush currents obtained for opening conditions which provide the maximum and minimum inrush current peaks for curve 1 i.e., 37.02 pu, 0.034 pu respectively

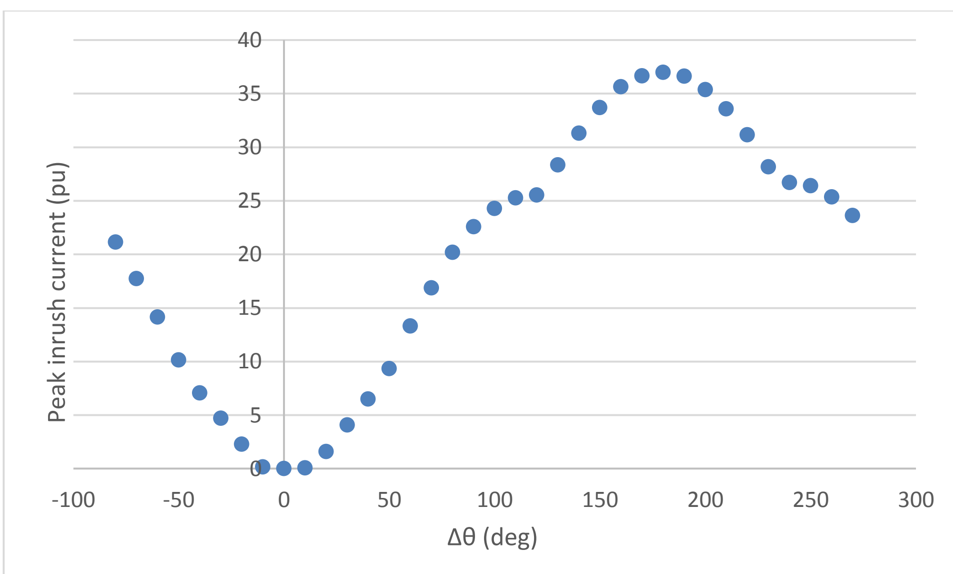

Figure 4.7 Peak inrush current for opening angle = 270 degrees

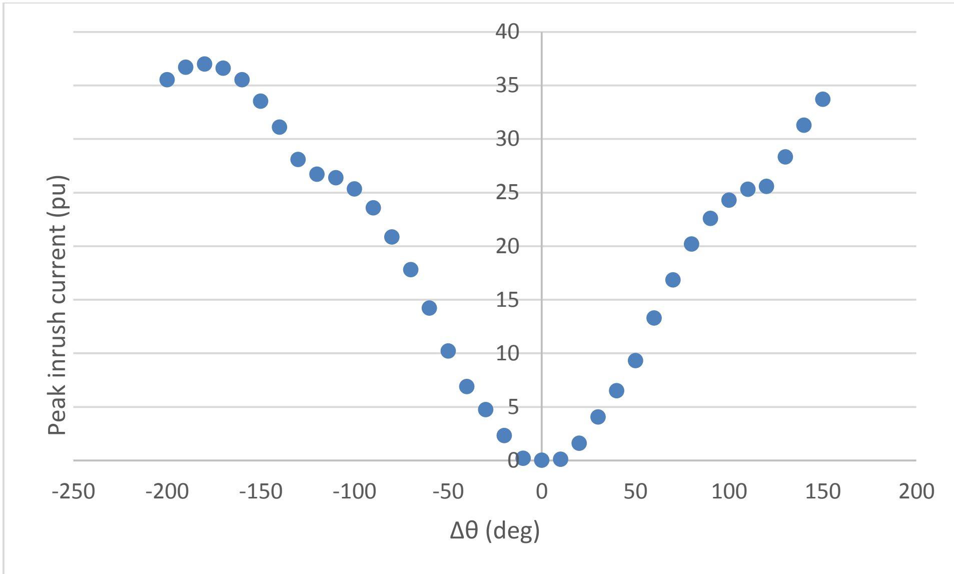

Figure 4.8 Peak inrush current for opening angle = 170 degrees

Curve 2:

Table 4.3 Saturation Characteristics curve 2

Current(A)	Flux (Vs)
0	0
0.000001	46.24
1.45	69.21
2.51	79.66
3.11	84.55
5.24	98.64
8.56	120.21
10.97	133.24
15.05	151.28
20.49	173.41
26.2	194.24
28.69	202.515
32.81	214.0913
36.81	222.54
41.95	231.363
53.59	244.37
65.62	251.031

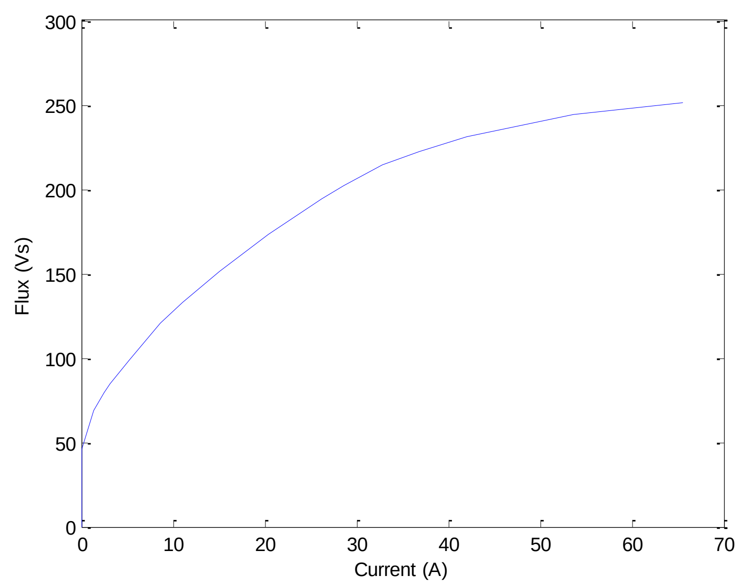

Figure 4.9 Saturation Curve for curve 2

Table 4.4 Opening at 90 degrees

Opening at 90 degrees	
Closing angle (deg)	Peak Inrush (pu)
0	0.79
30	0.53
60	0.39
90	0.37
120	0.39
150	0.53
180	0.80
210	0.94
240	1.12
270	1.18
300	1.14
330	0.94

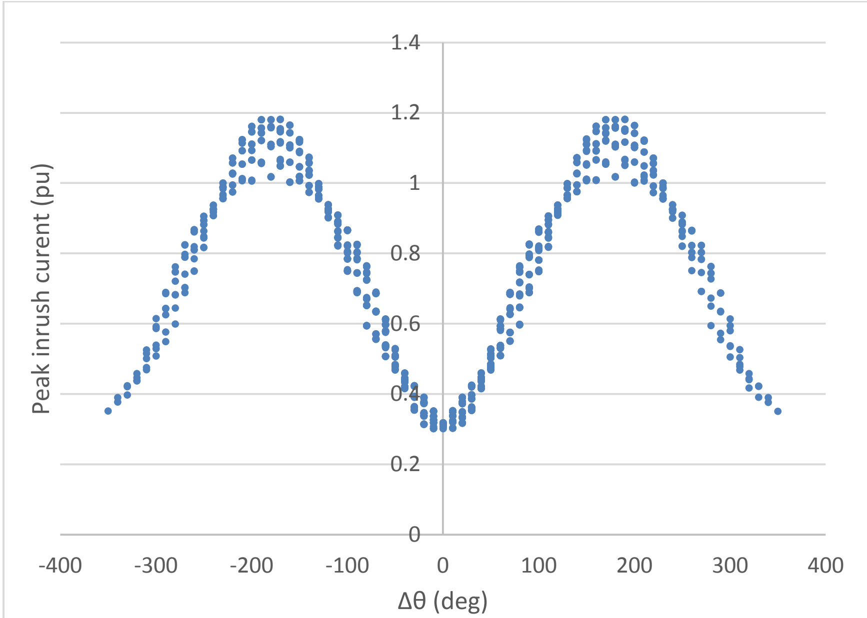

Figure 4.10 Δθ vs Peak inrush current

The results from Table 4.4 show that the least inrush is obtained by closing at the opening angle of 90 degrees. Figure 4.11 and Figure 4.12 illustrate the peak inrush currents obtained for opening conditions which provide the maximum and minimum inrush current peaks for curve 2 i.e., 1.18 pu, 0.302 pu respectively.

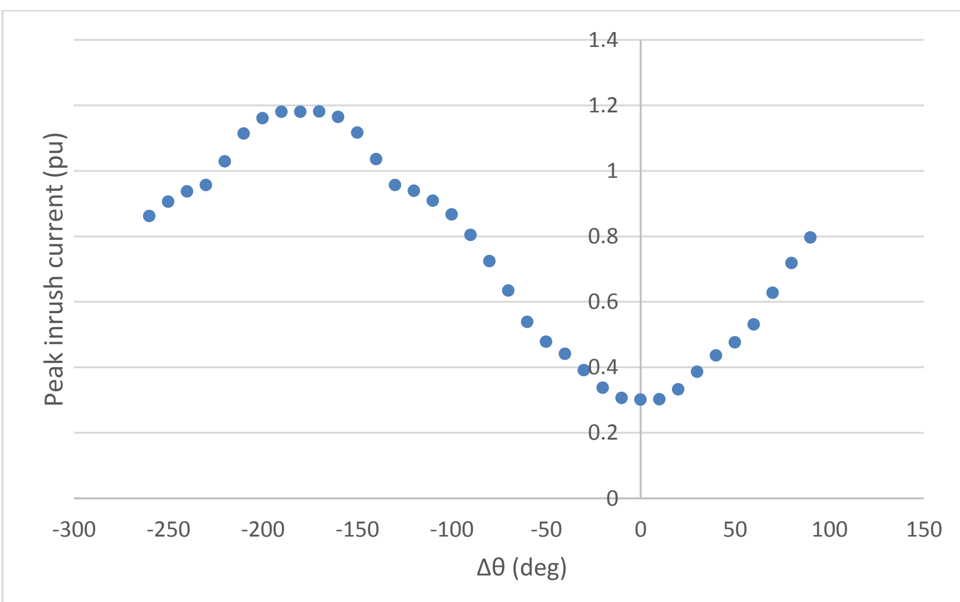

Figure 4.11 Peak inrush current for opening angle = 90 degrees

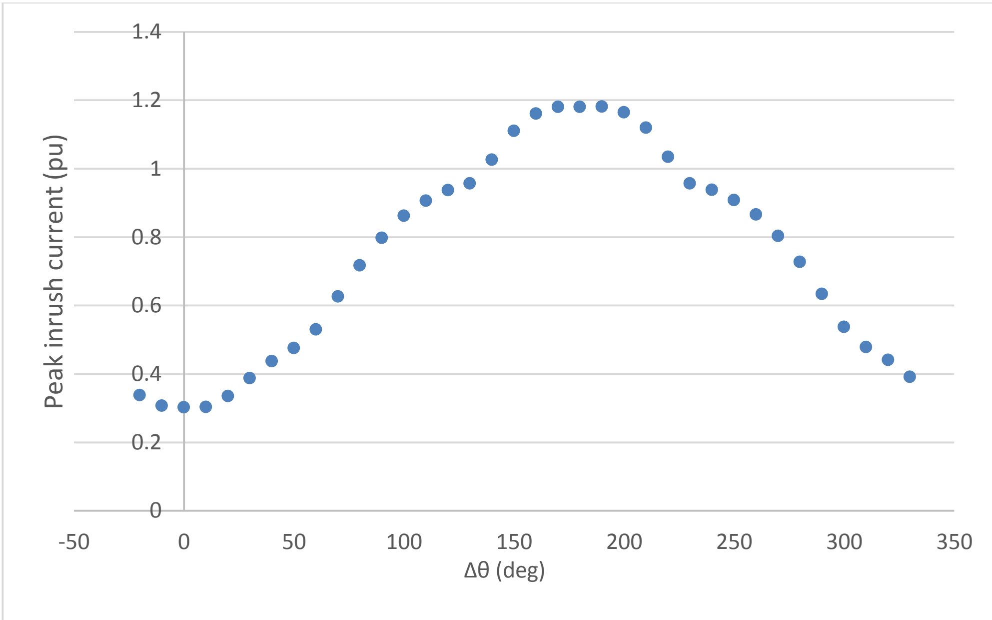

Figure 4.12 Peak inrush current for opening angle = 330 degrees

Curve 3:

Table 4.5 Saturation Characteristics curve 3

Current(A)	Flux (Vs)
0	0
0.000001	46.24
1.45	69.21
2.51	79.66
3.11	84.55
5.24	98.64
8.56	120.21
10.97	133.24
15.05	151.28
20.49	173.41
26.2	194.24
28.69	202.515
32.81	206.21
36.805	208.33
41.95	210.14
53.59	213.86
65.62	216.54

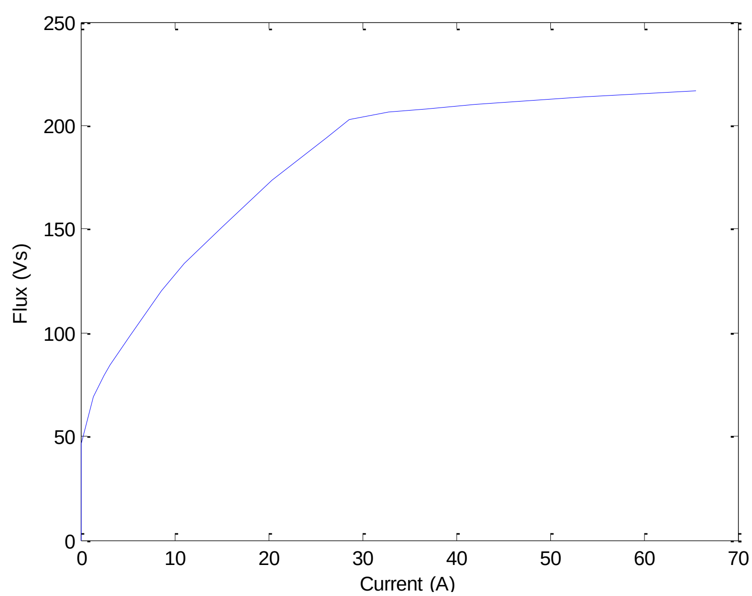

Figure 4.13 Saturation Curve for curve 3

Table 4.6 Opening at 30 degrees

Opening at 30 degrees	
Closing angle (deg)	Peak Inrush (pu)
0	2.55
30	0.01
60	2.69
90	8.59
120	14.49
150	16.58
180	21.48
210	23.57
240	21.43
270	16.46
300	14.32
330	8.39

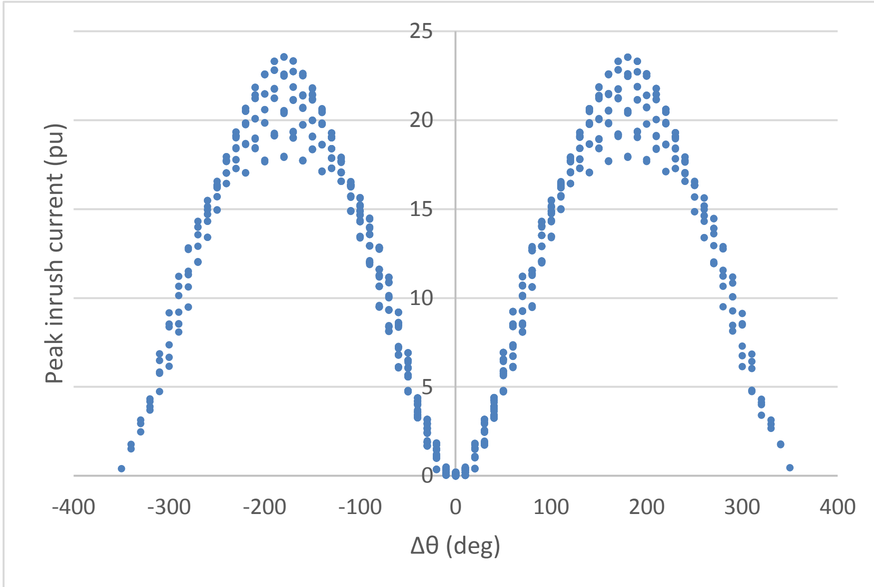

Figure 4.14 Δθ vs Peak inrush current

The results from Table 4.6 verifies that minimum inrush is obtained for the closing angle equal to the opening angle. Figure 4.15 illustrates the peak inrush current values for the opening angle of 30 degrees which produces maximum and minimum inrush current values of 23.57 pu and 0.01 pu respectively.

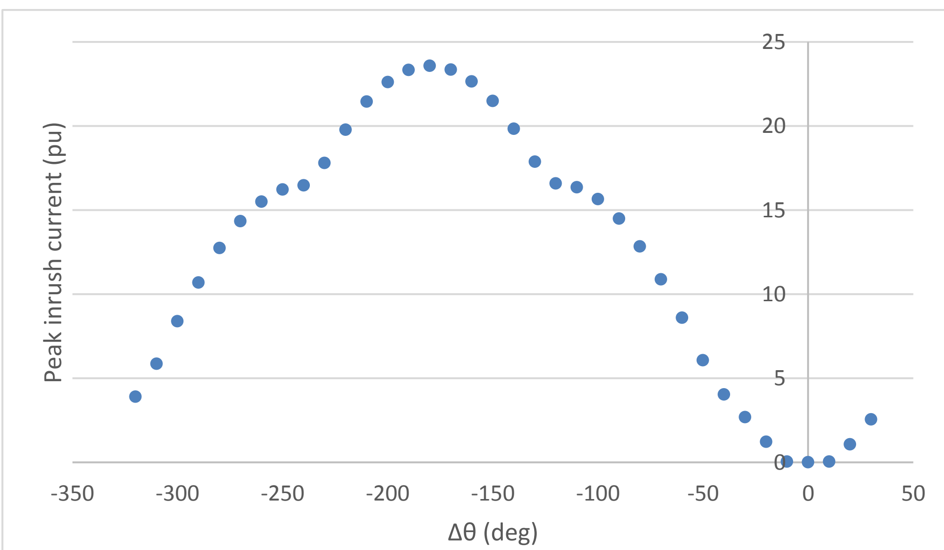

Figure 4.15 Peak inrush current for opening angle = 30 degrees

The slight randomness in inrush current calculations seen on the Figure 4.6 and Figure 4.10 is due to variation in the saturation characteristic input to the transformer (Table 4.1 and 4.3 respectively).

This section analyzed the impact of different core saturation characteristics on the gang-switching of transformer and it is seen from the above results that with the knowledge of the opening angle, the least inrush current for gang switching is obtained when closing at the opening angle, for all considered saturation characteristics whereas the calculations involved in the following section takes into account only the saturation characteristics in Table 3.2 applied across all the simulations in section 4.4.

4.4 Gang-switching for various transformer core and winding connections

The method of closing all the three phases simultaneously where the phase that is having the smallest residual flux equals to its prospective flux is analyzed in the following subsections. Real captured data will be used to evaluate the performance of this closing technique for different types of transformers and with different coupling methods. Due to uncertainty involved in the methodology for obtaining the optimal instants and variables involved that might impact in evaluating the optimal instants the derivative-free methods for minimizing non-convex functions are not used and instead the conventional method of brute force search is used so that all different conditions are taken into account and no optimal instant is missed. Also, one major disadvantage of using derivative-free methods such as Nelder-Mead and others is that the methods can take an enormous number of iterations increasing exponentially with negligible improvement in the functions nowhere reaching a minimum even for smooth, well-behaved functions. There is always a lack of convergence theory reflected on such algorithms. The brute force search method eliminates this theory.

The 10 test cases (Table A.1) or 11 test cases (Table A.2) were optimistically selected field data, captured real time and provided by the industry for the simulation exercise in such a manner that these test cases depict all the possible scenarios faced during real time transformer switching. All other random test cases that could be developed will only have an infinitesimal variation from one of the already used test case resulting in a similar argument leadings towards to the rule of thumb. As an illustration, in Table 4.8, test cases 2, 3 and 11 depict a scenario where there exists a high residual flux in one of the three phases. While test case 6 depicts a situation where the three-phase residual flux magnitudes are more or less balanced. This provides a sufficient validity on the usage of the specific test cases pertaining to the transformer configurations in the simulation. The test cases discussed are completely specified by the residual flux magnitudes and the geometrical configuration (three-legged or four-legged) only. The idea behind having these real test cases from the field was to run simulations with realistic information which is then mathematically illustrated and validated (Section 4.6).

4.4.1 Independent core transformer

This section details the simultaneous closing of all three breaker poles (gang operation) for various residual flux profiles obtained from actual field measurements carried out on a three-phase transformer (Delta-Y_g) with independent core configuration (three single-phase units)[29]. A three-phase transformer with three independent cores with a Delta winding either on primary or the secondary side can be used to simulate a three-legged core type transformer [31] justifying the three-legged residual flux data used for simulation purposes. The transformer is switched from the Delta side and the optimal angle of closing obtained for the different test cases considered is illustrated in the following plots. These angles were found by repetitive simulations exhausting all the possibilities of potential switching angles using a step search of 5 degrees, neither mechanical nor dielectric scattering was considered for the circuit breaker. For the transformer configuration used in this thesis, the interval of 5 degrees (0.23 ms interval for a 60Hz supply system) was chosen in such a way that substantially the optimal closing instants aren't missed during the simulation exercise. In the worst case (null flux), 0.23 ms corresponds to a vertical displacement of 8.724% on the voltage curve. This displacement is not high enough to miss a point of interest while evaluating closing instants. An interval of less than 5 degrees results in waste of simulation time and memory and those with larger interval resulted in optimal closing instants being missed. Table 4.7 shows the optimum closing angle for each assumed residual core flux profile, as found by repetitive trial and error simulations. All the residual flux scenario considered pertain to "flux-dependent" cases, i.e. the sum of all residual fluxes is zero. This can be justified by the presence of the Delta winding. Figure 4.16, Figure 4.17 illustrate the test case results with maximum and minimum peak inrush current magnitudes of Table 4.7.

Table 4.7 Gang operation results from three-phase independent core transformer with three-legged transformer residual flux data

Test #	Residual fluxes (PU)			Optimum closing angle (°)	Peak Inrush (A)
	RFA	RFB	RFC		
1	0.867	-0.683	-0.188	157	2.6781
2	-0.085	-0.064	0.149	55	303.71
3	-0.485	0.59	-0.102	325	56.293
4	-0.594	0.526	0.073	335	45.049
5	-0.539	0.296	0.242	345	99.828
6	0.835	-0.716	-0.119	155	1.4184
7	0.174	0.181	-0.355	250	195.23
8	-0.77	0.637	0.136	337	1.7649
9	-0.126	0.369	-0.244	280	177.69
10	-0.017	-0.281	0.299	80	202.41

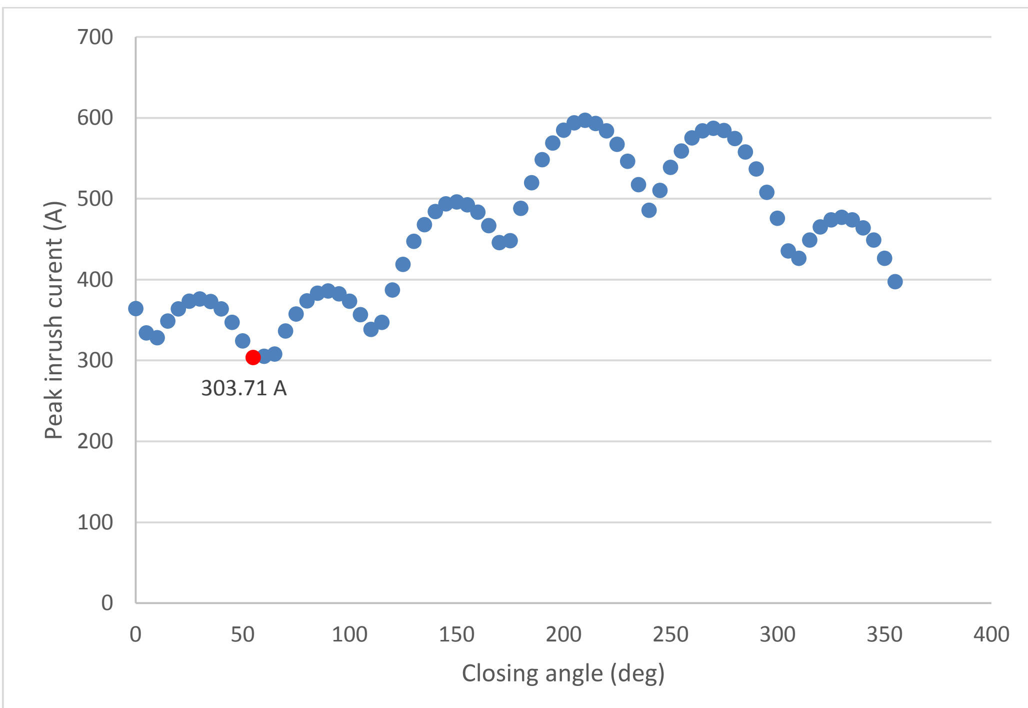

Figure 4.16 Test case 2 with highest peak inrush current among all test cases

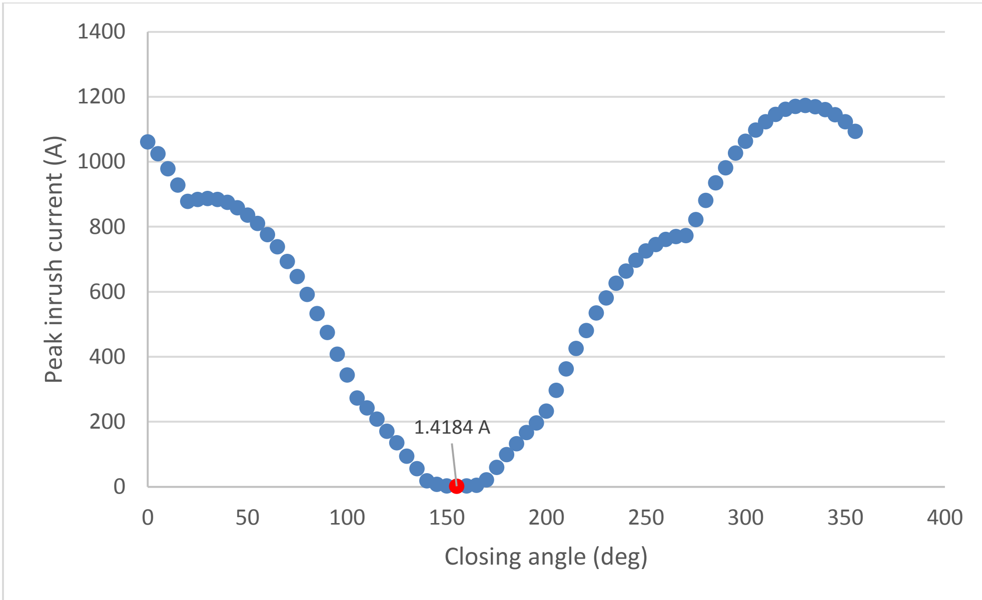

Figure 4.17 Test case 6 with lowest peak inrush current among all test cases

Figure 4.18, Figure 4.19, Figure 4.20 and Figure 4.21 illustrate the residual fluxes and prospective fluxes for cases #1, #6, #7 and #8 of Table 4.7 respectively. The black vertical lines illustrate the "optimal" switching instant for gang switching thus yielding the minimum possible inrush current.

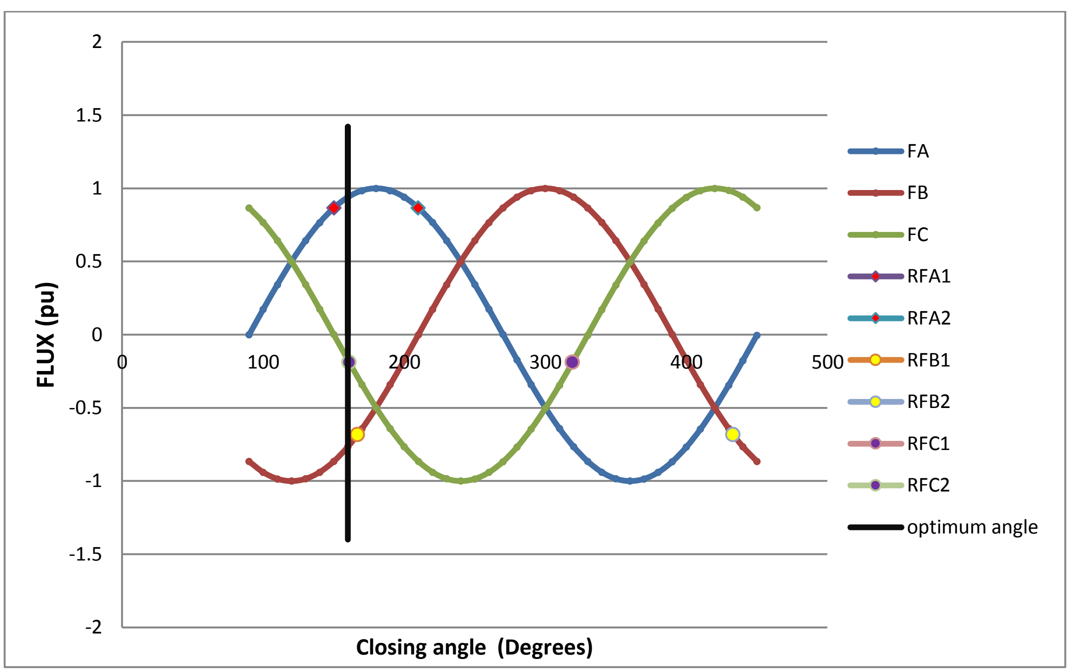

Figure 4.18 Test case 1 – Independent core transformer with three leg flux data

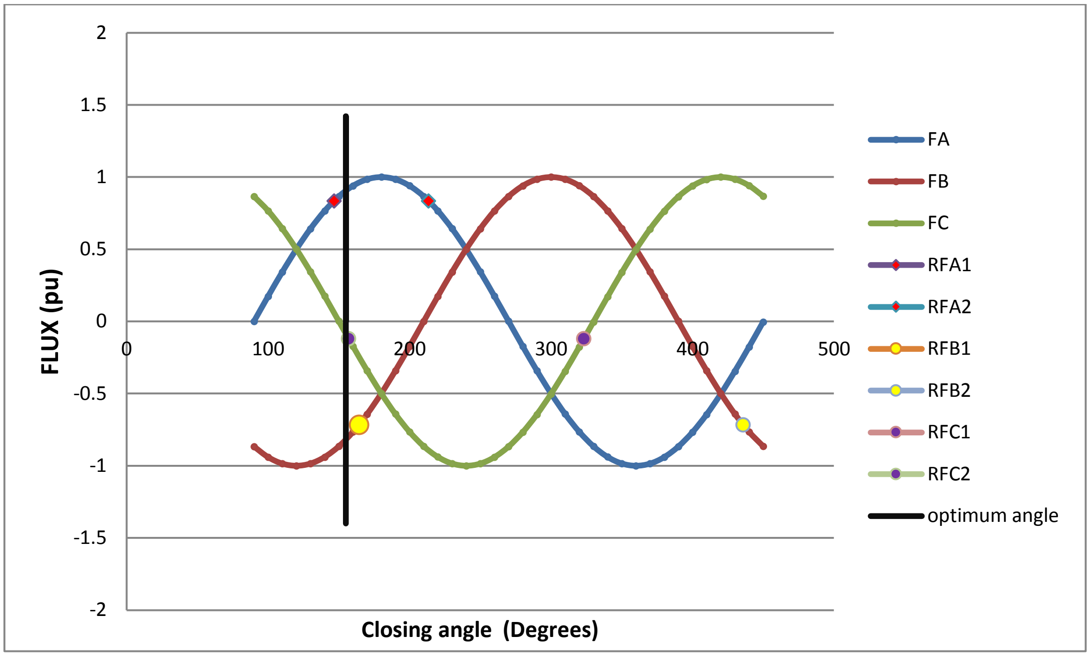

Figure 4.19 Test case 6 – Independent core transformer with three leg flux data

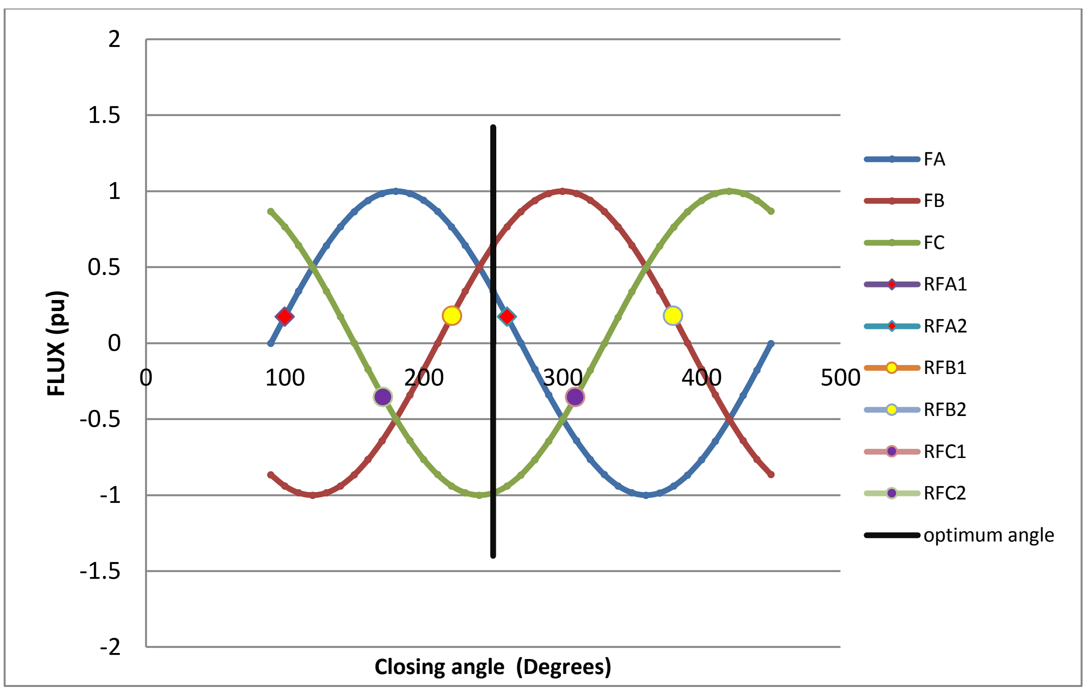

Figure 4.20 Test case 7 – Independent core transformer with three leg flux data

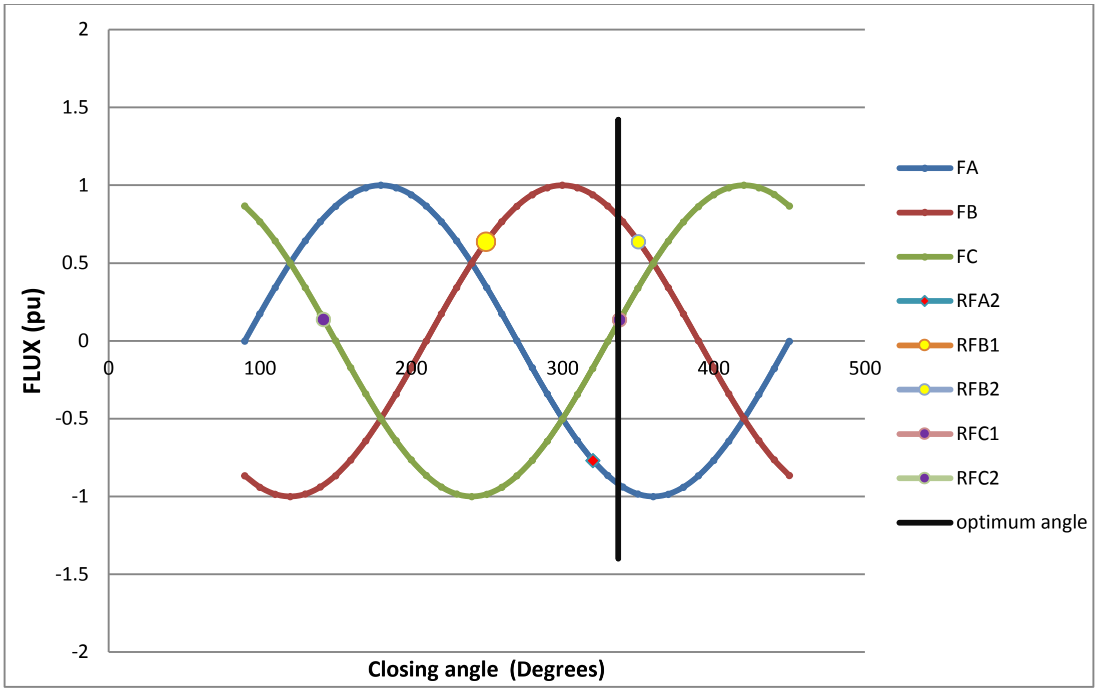

Figure 4.21 Test case 8 – Independent core transformer with three leg flux data

The least inrush current feasible for test case #2 found by exhaustive simulation search was 303.71 A and for test case #7 was 195.23 A. These currents are still considerably higher than the normal magnetizing current levels because the residual flux levels cannot match the prospective fluxes for all three phases no matter what switching angle is considered. The sub-optimal switching instant found, for any residual flux profile, is thus a compromise, inherent to the very physical constraints imposed by gang-switching.

The presence of the fourth leg in a four-legged transformer is for the imbalance which might pose a problem only when simulating independent pole switching strategies [21] unlike the gang switching strategy discussed in this chapter, justifying the four legged data being tested on three-legged core transformer models.

The following results and graphs below discuss the simulation of closing gang-operated circuit breakers using residual flux profiles from a four-legged transformer. The computer model used, however, was still three-phase transformer with independent cores [29]. Four-legged cores are characterized by the fact that the residual fluxes for the wounded phase legs do not sum up to zero, since there will be some flux in the outer higher reluctance core leg containing no winding. Residual flux profiles of this type are shown in Table 4.8 and they were obtained from an actual four-legged transformer. The methodology of exhaustive simulation searches, carried out for the previous case was also followed here as well. Figure 4.24-Figure 4.27 illustrate some of the typical results for few test cases. Figure 4.22 and Figure 4.23 illustrate the test case results with maximum and minimum peak inrush current magnitudes of Table 4.8. From the table it can be seen that the maximum inrush current value is 198.36 A for Test case 6 which still far exceeds steady state magnetizing current levels, meaning that the found closing point is sub-optimal. Still, however, controlled switching is valuable in this scenario too as the worst case inrush current will be 810.39 A under random closing conditions.

Table 4.8 Gang operation results from three-phase independent core transformer with four legged residual flux data

Test #	Residual fluxes (PU)			Optimum closing angle (°)	Peak Inrush Current (A)
	RFA	RFB	RFC		
1	0	0.084	-0.597	240	129.62
2	0.302	0.233	-0.831	235	37.439
3	-0.483	0.653	-0.744	280	39.575
4	-0.552	0.481	-0.282	330	76.369
5	-0.575	0.239	0.36	15	80.841
6	-0.194	0.262	-0.311	260	198.36
7	-0.053	-0.505	0.784	75	6.728
8	0.207	-0.548	0.822	85	46.437
9	0.586	-0.557	0.473	150	75.886
10	0.519	-0.722	0.599	105	18.968
11	0.941	-0.945	0.552	130	7.4507

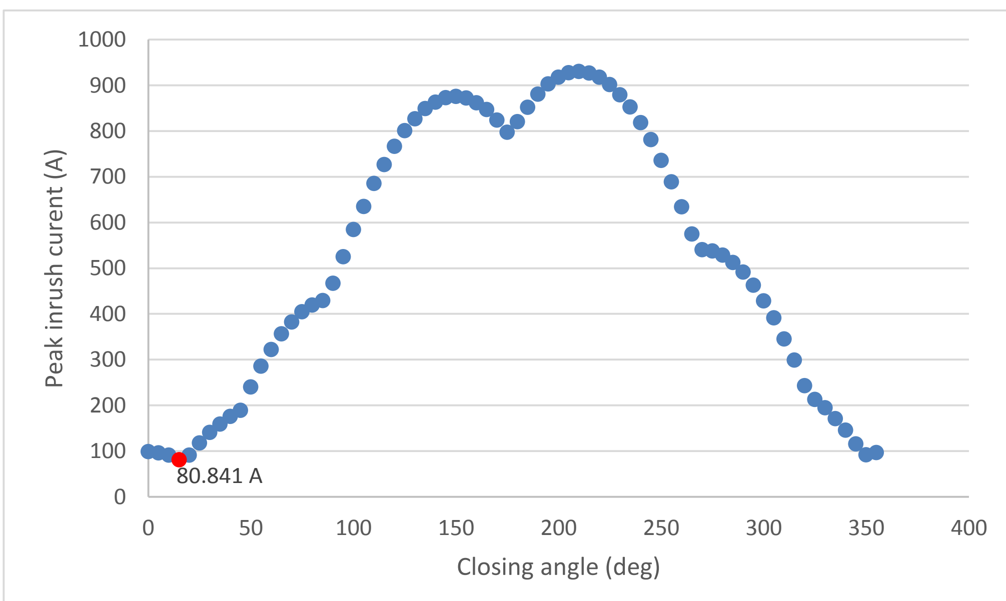

Figure 4.22 Test case 5 with highest peak inrush current among all test cases

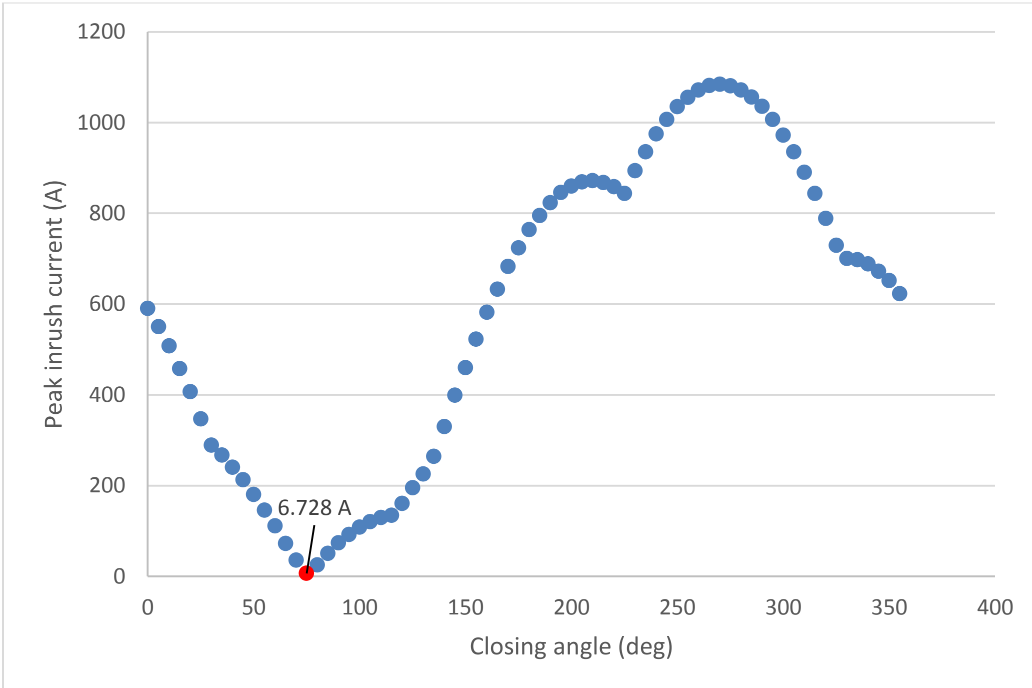

Figure 4.23 Test case 7 with lowest peak inrush current among all test cases

The vertical lines in the following graphs illustrate the "optimal" switching instant for all three phases yielding the minimum possible inrush current.

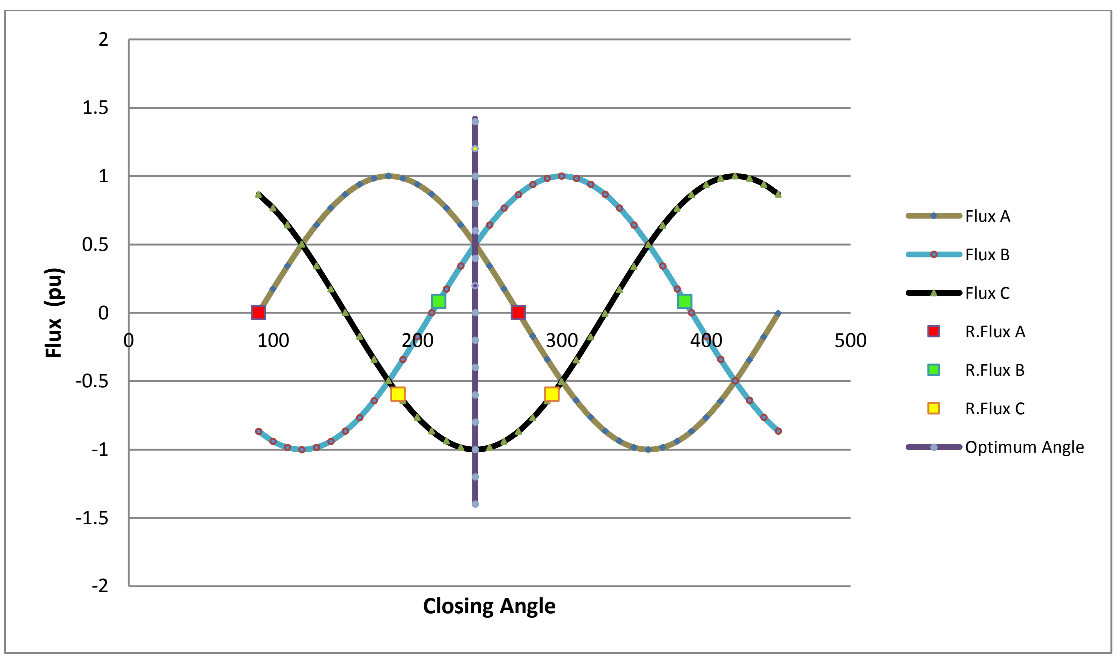

Figure 4.24 Test case 1 – Independent core transformer with four leg flux data

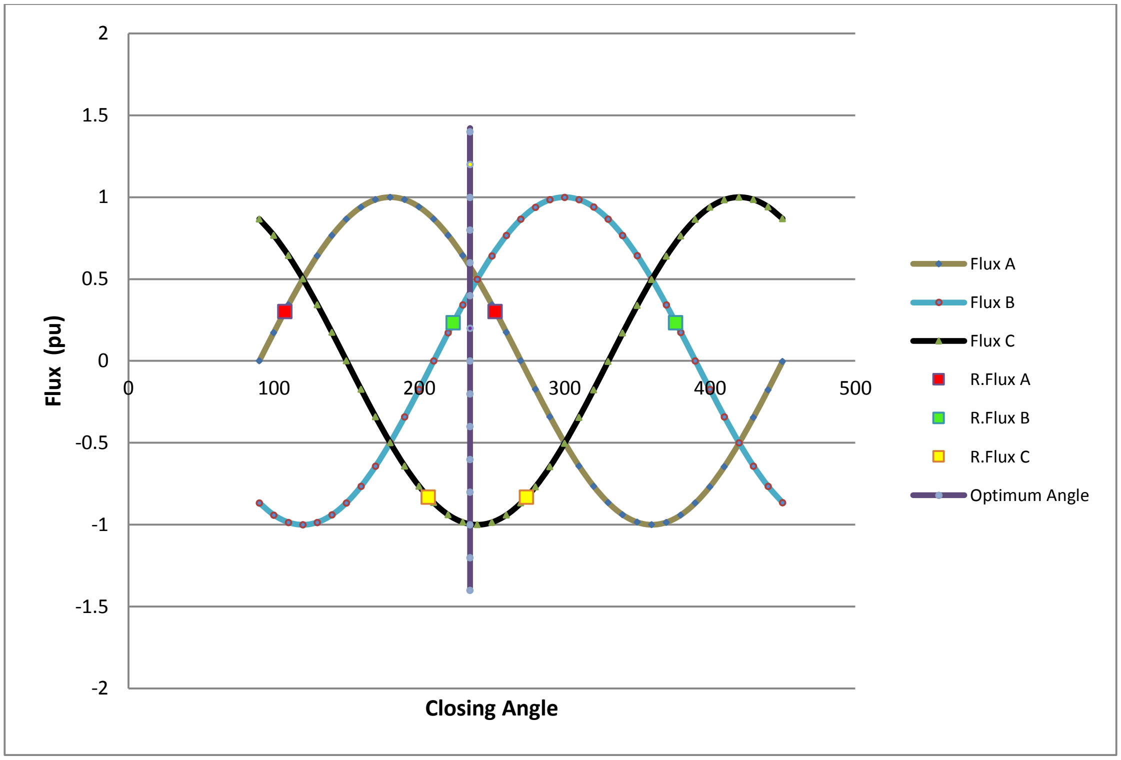

Figure 4.25 Test case 2 – Independent core transformer with four leg flux data

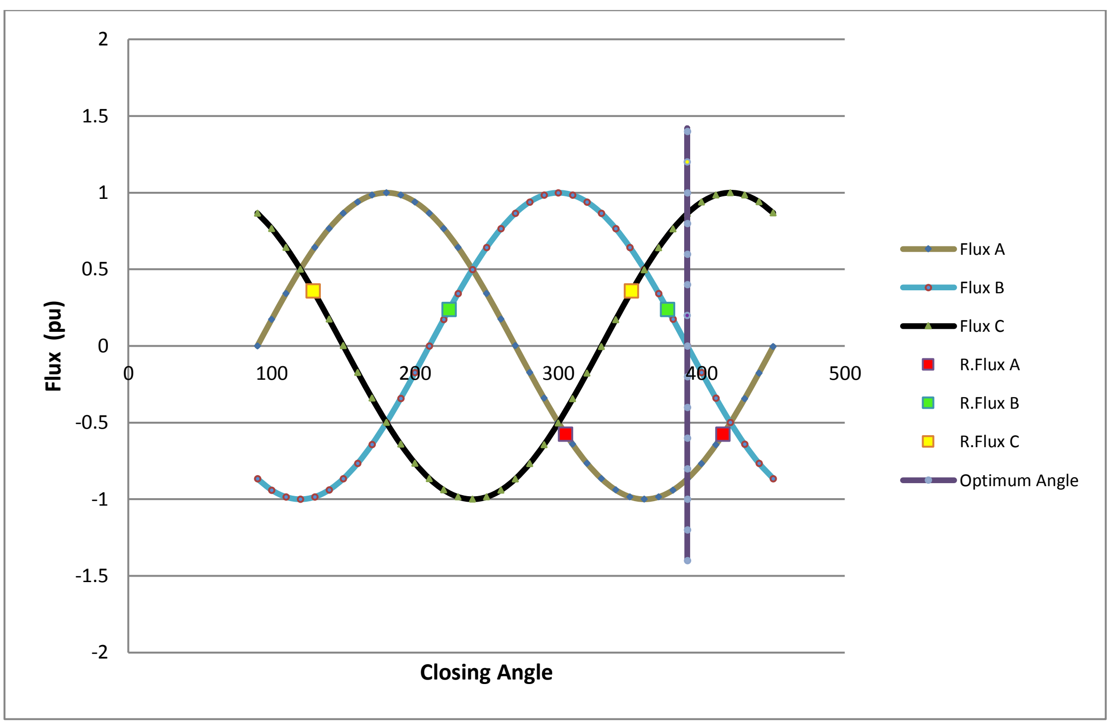

Figure 4.26 Test case 5 – Independent core transformer with four leg flux data

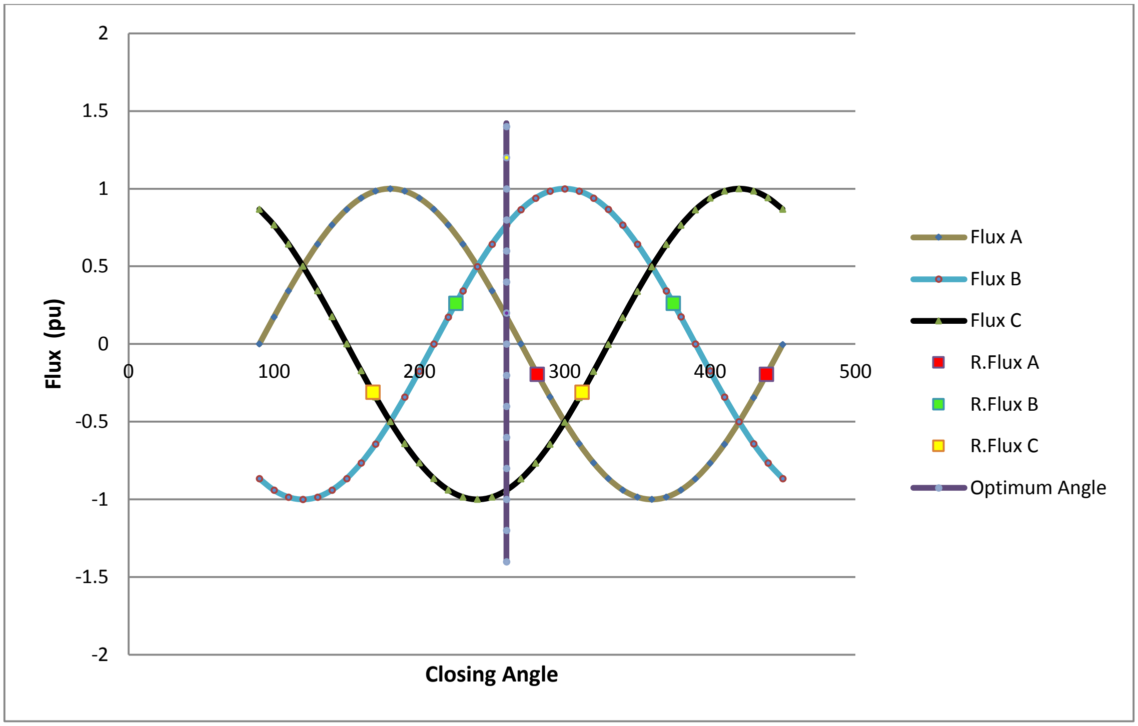

Figure 4.27 Test case 6 – Independent core transformer with four leg flux data

The observation that the optimal switching instant to be the moment at which the angle of the phase that has the smallest residual flux equals its prospective flux in absolute magnitude is seen to be still reasonably valid even for this set of residual flux data.

4.4.2 Three-legged core type transformer

This section deals with gang-operated transformer switching performed in a three-legged core type three-phase transformer discussed in section 3.4. The core exhibits magnetic coupling between the phases. The field obtained residual flux data are used in the simulations [A.1]. The obtained results, following the same methodology of exhaustive simulation searches, along with the already obtained results from three independent core configuration are summarized in Table 4.9.

Table 4.9 Gang operation results from three-legged core type transformer with three-legged residual flux data

Test #	Residual fluxes (PU)			Optimum closing angle (deg) (Core type transformer)	Optimum closing angle (deg) (Three single-phase transformers)	Difference (deg)
	RFA	RFB	RFC			
1	0.867	-0.683	-0.188	157	157	0
2	-0.085	-0.064	0.149	110	55	55
3	-0.485	0.59	-0.102	315	325	10
4	-0.594	0.526	0.073	325	335	10
5	-0.539	0.296	0.242	330	345	15
6	0.835	-0.716	-0.119	155	155	0
7	0.174	0.181	-0.355	280	250	30
8	-0.77	0.637	0.136	330	337	7
9	-0.126	0.369	-0.244	295	280	5
10	-0.017	-0.281	0.299	110	80	30

From the above results it can be seen that the optimum angle for getting the least inrush current in core type transformer is very close to the one obtained for a three-phase transformer composed of three independent cores. The slight variation seen in the results is due to: a) the presence of the magnetic coupling in the core type as well as the usage of a different saturation curve and b) a different saturation curve used for the three-legged core to ensure simulation consistency between the field-obtained residual flux data of the three-legged transformer and its actual manufacturer recommended magnetic characteristics.

The subsequent results in Table 4.10 discuss the simulation of gang operation using the field data obtained from four-legged transformers on a three legged core configuration by virtue of the same methodology used in the previous simulations. The particularity of the four-legged core is that despite the presence of the Delta winding, that restricts the phase leg fluxes to add up to zero during operation, the residual flux profile does not have to satisfy this constraint due to the existence of the fourth leg. The table also compares the results with those obtained from independent core transformer. The results indicate that the discrepancy between the closing angles is not significant and in the same order of magnitude as the difference experienced due to a different core saturation characteristic for the three-legged core simulations.

Table 4.10 Gang operation results from three-legged core type transformer with four-legged residual flux data

Test #	Residual fluxes (PU)			Optimum closing angle (deg) (Independent core transformer)	Optimum closing angle (deg) (four-legged Core structure)	Difference (deg)
	RFA	RFB	RFC			
1	0	0.084	-0.597	240	260	20
2	0.302	0.233	-0.831	235	250	15
3	-0.483	0.653	-0.744	280	290	10
4	-0.552	0.481	-0.282	330	320	10
5	-0.575	0.239	0.36	15	335	40
6	-0.194	0.262	-0.311	260	295	35
7	-0.053	-0.505	0.784	75	85	10
8	0.207	-0.548	0.822	85	100	15
9	0.586	-0.557	0.473	150	130	10
10	0.519	-0.722	0.599	105	120	15
11	0.941	-0.945	0.552	130	135	5

4.4.3 Different winding connections in three-legged core type transformer

The Gang operation of the three-phase three-legged core type structure was carried out for different configurations of the switched winding and the optimum closing angle was evaluated for all considered residual flux profiles, obtained from a three-legged transformer. The results shown in Table 4.11, indicate that the optimum angle is the same for Y_g-Y_g, Y-Y and D-Y_g connections. The magnitude of the inrush currents is, however, different for different winding connections.

The results obtained in Table 4.11 suggest the following "rule of thumb" can be applied;

For a given gang-operated transformer with residual flux values measured, the optimum closing angle for a given residual flux profile is the angle of the phase that has the smallest residual flux in absolute magnitude which will provide the least inrush current. As an illustration, a reference to Figure 4.19 will show that residual flux in Phase C has least absolute value and the optimum closing angle is across that point.

Table 4.11 Gang operation in three-legged core type transformer for different configuration (Three-legged case)

Test #	Residual fluxes (PU)			Optimum closing angle (deg)	Peak Inrush current (A) (D-Yg)	Peak Inrush current (A) (Yg-Yg)	Peak Inrush current (A) (Y-Y)
	RFA	RFB	RFC				
1	0.867	-0.683	-0.188	157	78.123	86.431	52.486
2	-0.085	-0.064	0.149	110	208.84	220.21	183.31
3	-0.485	0.59	-0.102	315	120.75	132.59	95.21
4	-0.594	0.526	0.073	325	121.78	133.59	96.029
5	-0.539	0.296	0.242	330	154.89	166.24	128.32
6	0.835	-0.716	-0.119	155	77.548	85.883	52.516
7	0.174	0.181	-0.355	280	182.51	193.4	156.29
8	-0.77	0.637	0.136	330	95.227	104.62	65.944
9	-0.126	0.369	-0.244	295	156.75	167.25	132.22
10	-0.017	-0.281	0.299	110	166.43	177.3	144

4.5 EMTP- RV and MATLAB results for Gang-switched transformer banks

Results from EMTP-RV [33] are discussed in the following section. Figure 4.28 illustrates the inrush current magnitudes versus $\Delta\theta$, i.e., the angle difference between the opening and the closing angle. Figure 4.29 depicts, for any value of the opening angle on the X-axis, the inrush currents obtained for various closing angles on the Y-axis. Figure 4.30, in turn, depicts for any value of the closing angle on the X-axis, the inrush currents obtained for various opening angles on the Y-axis. The results pertain to three independent cores constituting a three-phase transformer unit.

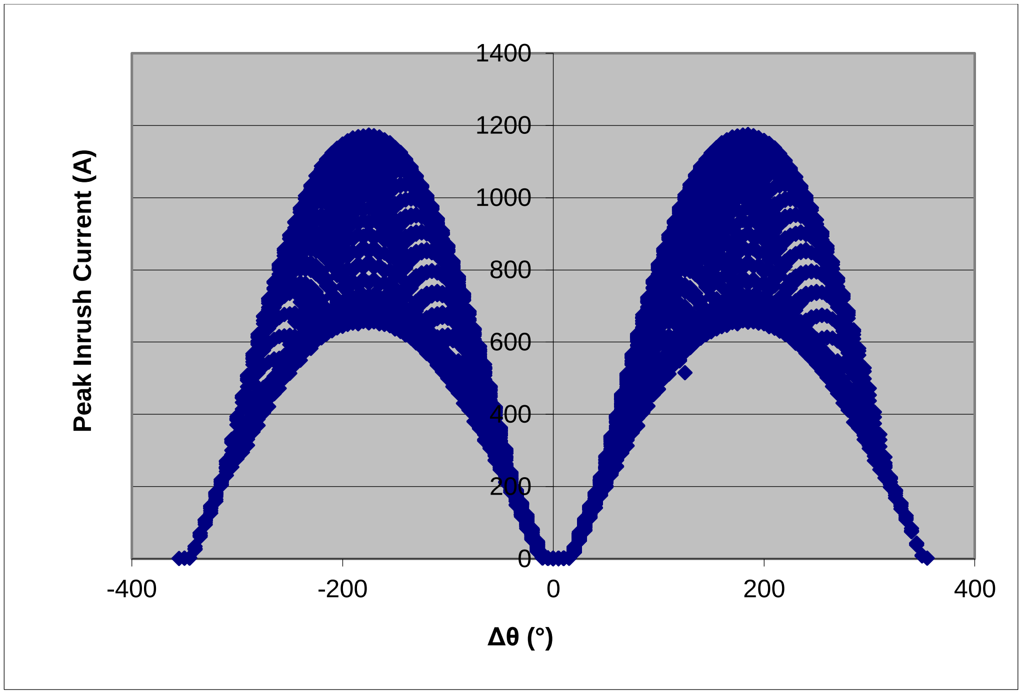

Figure 4.28 The angle difference Δθ versus the Peak inrush current from EMTP [33]

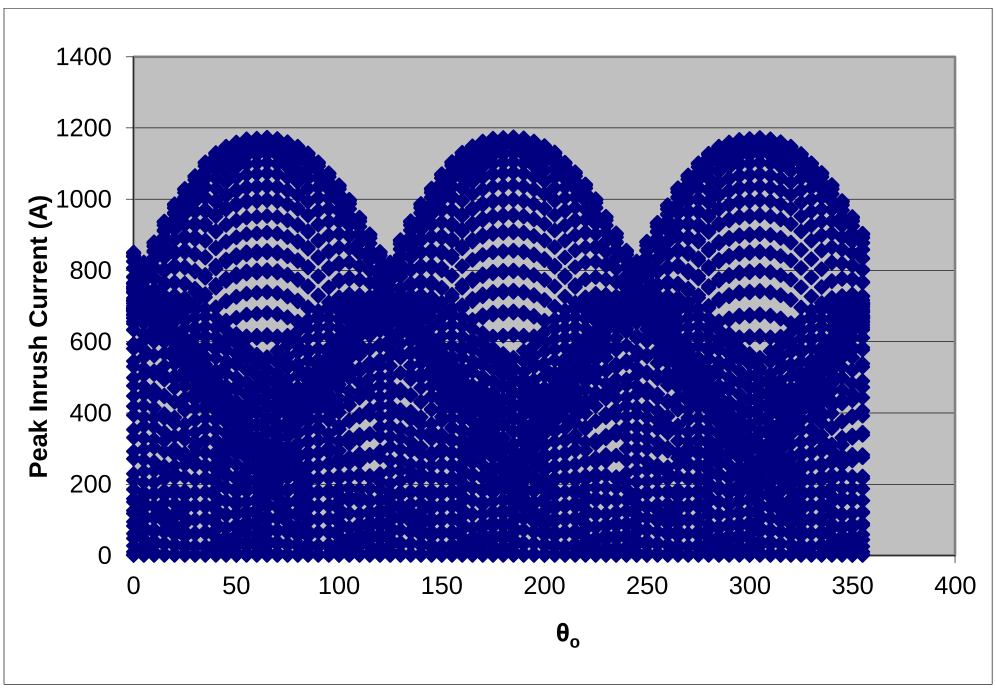

Figure 4.29 The opening angle θ_o versus the Peak inrush current from EMTP [33]

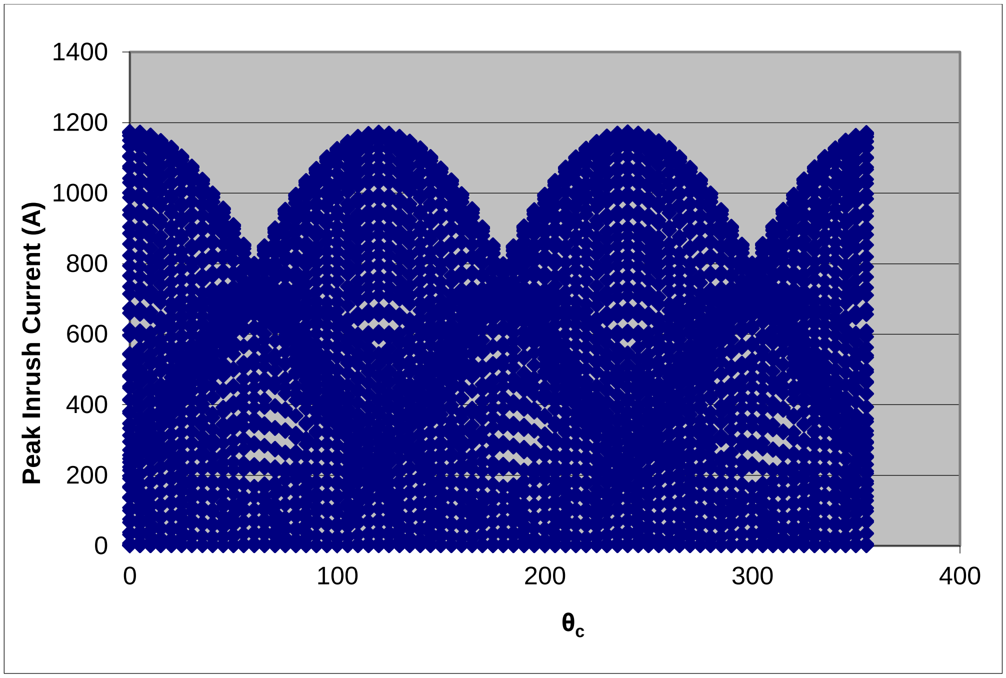

Figure 4.30 The closing angle θ_c versus the Peak inrush current from EMTP [33]

Similar results to the ones shown in Figure 4.28, were obtained in this thesis using the SimPowerSystems environment and are illustrated in Figure 4.31.

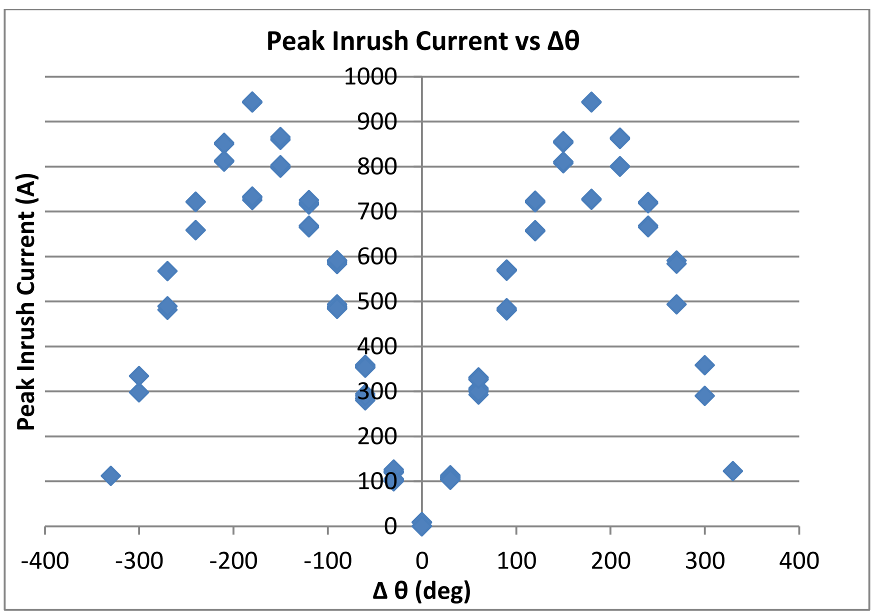

Figure 4.31 The angle difference $\Delta\theta$ versus the Peak inrush current from SIMULINK

Sample tabular results used to generate Figure 4.28 and Figure 4.31 are shown in Table 4.12(a). More detailed first-peak magnitude inrush currents as a function of different closing angles and for particular opening angles are given in Tables 4.12(b) and 4.12(c). Tables 4.12(b) and 4.12(c) generated from MATLAB/Simulink also illustrate, for a given opening (disconnection) angle the peak inrush currents that would have been obtained had the switching occurred at the tabulated angles.

Table 4.12 (a) $\Delta\theta$ vs Peak inrush current for SIMULINK & EMTP

Δθ	Peak inrush current (A) - SIMULINK	Peak inrush current (A) - EMTP
0	0.7395	1.415
30	120.75	97.47
60	355.46	273.254
90	590.34	458.6
120	669.08	744.35
150	866.28	1038.75
180	944.85	1172.07

4.5.1 Comparison of graphs (SIMULINK SimPowerSystems vs EMTP)

From Table 4.12 (a), it can be seen that the maximum value of inrush current in the SimPowerSystems environment was found to be 944.85 A. However, a current of 1172.07A was found when using the EMTP-RV model. The results are in qualitative agreement and show that for both simulation environments: a) the peak inrush current is minimized whenever the opening and closing angles coincide and b) the peak inrush currents are maximized whenever the opening and closing angle differ greatly. In terms of quantitative comparison, the variation is approximately 19.3% and is traced to the fact that the EMTP-RV simulations were conducted using three hysteretic reactors simulated each with its own magnetic characteristic in the form of an actual hysteresis loop, while the MATLAB simulations used magnetic cores exhibiting magnetic characteristics in the form of piece-wise linear lines. The difference in the core modeling was ostensibly retained to assess its quantitative effect.

Table 4.12(b) Opening angle 120 degrees

Opening angle = 120 degrees	
Closing Angle (degrees)	Peak Inrush Current (A)
0	723.29
30	481.27
60	307.4
90	113.78
120	9.4256
150	101.77
180	280.41
210	483.98
240	718.24
270	798.11
300	733.49
330	813.42

Table 4.12(c) Opening angle 30 degrees

Opening angle = 30 degrees	
Closing Angle (degrees)	Peak Inrush Current (A)
0	104.89
30	0.75438
60	119.6
90	353.21
120	587.62
150	665.68
180	859.48
210	943.22
240	853.43
270	658.84
300	567.68
330	334.67

The simulations which were discussed in section 4.3 further supports the idea of closing the gang switched transformer same as the opening angle which results in the least inrush current.

4.6 An alternative approach for Gang-switching

The brute force search method of finding the optimal closing instant discussed in section 4.4, although time consuming, has been useful in determining the above-stipulated simplified rule that permits advantageous simultaneous closing for three-phase transformers. From the brute force search technique the optimal point at which the gang operation is feasible for minimum inrush current is obtained and optimally/sub-optimally the best choice of closing instant would be to close at the dynamic flux equalization point of the phase possessing the minimum residual flux near the prospective flux value. This can be seen in Table 4.13, where tests were performed on the three-legged independent core type transformer (Delta-Y_g). This approach can be seen as a mathematical interpretation of the brute force search approach. A more accurate, but more computationally intensive, version of the simplified closing rule, yielding results closer to those obtained using the brute force technique can be formulated as follows:

Let φ_{Pe} and φ_{Re} be the prospective flux and residual flux of phase "e" respectively. The objective would be to minimize the sum of differences between φ_{Re} and $\varphi_{Pe}(t_{u+i})$ where i corresponds to the window of angular space to minimize the objective function. Here, i varies from 0 degrees to 359 degrees. The optimum angle can be obtained from previous method by minimizing the objective function with t_u equal to the angle at which smallest residual flux equals its prospective flux and i varied from -30 degrees and +30 degrees. This will in turn reduce the computational time as compared to minimizing for a whole cycle of 360 degrees. The closing instant algorithm is mathematically represented as follows,

$$Min \sum_{i=0}^{359} \sum_{e=a,b,c} \varphi_{Pe}(t_{u+i}) - \varphi_{Re} \qquad (4.1)$$

Table 4.13 Comparison of Brute Force search vs Closing Instant Algorithm – Independent core type transformer

Test #	Residual fluxes (PU)			Minimum inrush current (A)		Optimum Closing Angle (deg)		Optimal Phase from Brute Force Search	Optimal Phase from Closing instant Algorithm
	RFA	RFB	RFC	Brute Force Search	Closing instant Algorithm	Brute Force Search	Closing instant Algorithm		
1	0.867	-0.683	-0.188	2.6781	2.6791	157	161	C	C
2	-0.085	-0.064	0.149	303.71	486.4633	55	85	B	C
3	-0.485	0.59	-0.102	52.121	52.1366	325	324	C	C
4	-0.594	0.526	0.073	41.905	41.9675	335	334	C	C
5	-0.539	0.296	0.242	96.322	97.9011	345	344	C	C
6	0.835	-0.716	-0.119	1.4184	1.5812	155	157	C	C
7	0.174	0.181	-0.355	195.23	213.7182	250	220	A	A
8	-0.77	0.637	0.136	1.7649	1.9833	337	338	C	C
9	-0.126	0.369	-0.244	177.69	184.2952	280	277	A	A
10	-0.017	-0.281	0.299	202.41	209.1931	80	89	A	A

Table 4.13 demonstrates that the closing instants and optimum closing angles recommended by the rule of thumb are close to those found analytically by the suggested closing instant algorithm. The inrush currents obtained using the alternative closing approach do not exhibit a major difference when compared with the ones obtained from the brute force search approach. The disparity found in Test case 2 is due to the specific residual flux profile wherein the per phase optimal switching points are located far from one another thus making both Phase B and Phase C a viable optimal phase for closing. This disparity in test case #2 was also found with the three-legged core type transformer simulation results as shown in Table 4.14.

Table 4.14 Comparison of Brute Force search vs Closing Instant Algorithm – Three-legged core type transformer

Test #	Residual fluxes (PU)			Minimum inrush current (A)		Optimum Closing Angle (deg)		Optimal Phase from Brute Force Search	Optimal Phase from Closing instant Algorithm
	RFA	RFB	RFC	Brute Force Search	Closing instant Algorithm	Brute Force Search	Closing instant Algorithm		
1	0.867	-0.683	-0.188	76.123	78.854	157	170	C	C
2	-0.085	-0.064	0.149	208.84	295.378	110	55	B	C
3	-0.485	0.59	-0.102	120.75	129.87	315	305	C	C
4	-0.594	0.526	0.073	121.78	135.77	325	335	C	C
5	-0.539	0.296	0.242	154.89	162.21	330	318	C	C
6	0.835	-0.716	-0.119	77.548	84.98	155	145	C	C
7	0.174	0.181	-0.355	182.51	190.63	280	295	A	A
8	-0.77	0.637	0.136	95.227	110.56	330	335	C	C
9	-0.126	0.369	-0.244	156.75	175.32	295	275	A	A
10	-0.017	-0.281	0.299	166.43	181.654	110	100	A	A

This method can be considered as an analytical interpretation of the rule of thumb with the difference that this approach takes into account the minimization of sum of the difference between the prospective and residual flux in all three phases whereas the rule of thumb considers only the phase with minimum residual flux value into account.

Chapter 5 Conclusions and Future Research

5.1 Summary

In this thesis a controlled point-on-wave switching strategy to minimize inrush currents for gang operated circuit breakers employed in distribution transformers is tested in simulation. Two switching cases were analyzed.

The first scenario dealt with deducing the optimum closing angle to minimize inrush currents when the instant of de-energization (i.e., opening angle) is known. The simulation results obtained via Matlab SimPowerSystems were similar to the results obtained independently in EMTP-RV by other researchers.

The second scenario dealt with evaluation of the optimum closing angle with a prior knowledge of residual flux profile of the three-phase transformer. Field obtained residual flux data was used and the optimum closing angle for minimum inrush current is suggested by two different methods which were tested on different transformer core configurations, geometric constructions and winding connections.

5.2 Conclusion

The following were conclusions from the analysis of simulations elucidated in this thesis,

- The first approach suggests to close the gang operated circuit breaker on the phase with smallest residual flux equaling its prospective flux
- The second approach proposes a mathematical formulation for obtaining the optimal closing instant by minimizing for all three phases, the sum of difference between the prospective flux values and corresponding residual flux in one cycle.
- The gang operated closing strategy for least inrush current with the knowledge of the de-energization angle is found to be same as the opening angle. This strategy provided at least 98.1% less inrush current as compared to inrush currents due to a random

energization. This strategy provided least inrush currents when tested with different core saturation characteristics thus was found to be a reliable strategy in such given conditions.

- The gang operated closing strategy for least inrush current with the knowledge of the three-phase residual flux profile is to close the circuit breaker at the point where the smallest residual flux equals its prospective flux as suggested by the rule of thumb (first approach) which was found to provide 84% lesser inrush currents than a random energization for a worse case residual flux profile.

- The analytical approach proposed also proved to obtain minimum inrush currents similar to results obtained from the rule of thumb which suggests as a viable gang operated closing strategy.

- Both these methods being validated on several transformer core configurations and winding connections with credible residual flux profile information, performed effectively in reducing the inrush currents and prove worthy as a cost effective gang operated closing strategy for low cost distribution transformers where cost of new protective equipment is non-feasible.

5.3 Recommendations for future work

In this thesis ideal circuit breakers are used in the simulations for switching. To further investigate/solidify the suggested approaches, the circuit breaker can be modelled using the Cassie and Mayr arc models.

Appendix A

A.1 Residual flux field measured data

Table A.1 Three legged transformer residual flux data

Residual fluxes (pu)		
RFA	RFB	RFC
0.867	-0.683	-0.188
-0.085	-0.064	0.149
-0.485	0.59	-0.102
-0.594	0.526	0.073
-0.539	0.296	0.242
0.835	-0.716	-0.119
0.174	0.181	-0.355
-0.77	0.637	0.136
-0.126	0.369	-0.244
-0.017	-0.281	0.299

Table A.2 Four legged transformer residual flux data

Residual fluxes (pu)		
RFA	RFB	RFC
0	0.084	-0.597
0.302	0.233	-0.831
-0.483	0.653	-0.744
-0.552	0.481	-0.282
-0.575	0.239	0.36
-0.194	0.262	-0.311
-0.053	-0.505	0.784
0.207	-0.548	0.822
0.586	-0.557	0.473
0.519	-0.722	0.599
0.941	-0.945	0.552

A.2 Matlab implementation of opening and closing angles

Opening at 30 deg and Closing at 240 deg

Figure A.1 CB Control signal & Voltage Phase Angle periodic variation illustrates the way to circumvent giving the MATLAB an actual command in the time domain. Instead, the command is given using as input the actual opening and closing angles. The lower part of the graph contains the triangular periodic waveform, each triangle corresponding to the varying voltage angle per period (16ms for the 60 Hz supply used here). The upper part of the graph illustrates the time the open and close commands are given vis a vis the desired voltage angles.

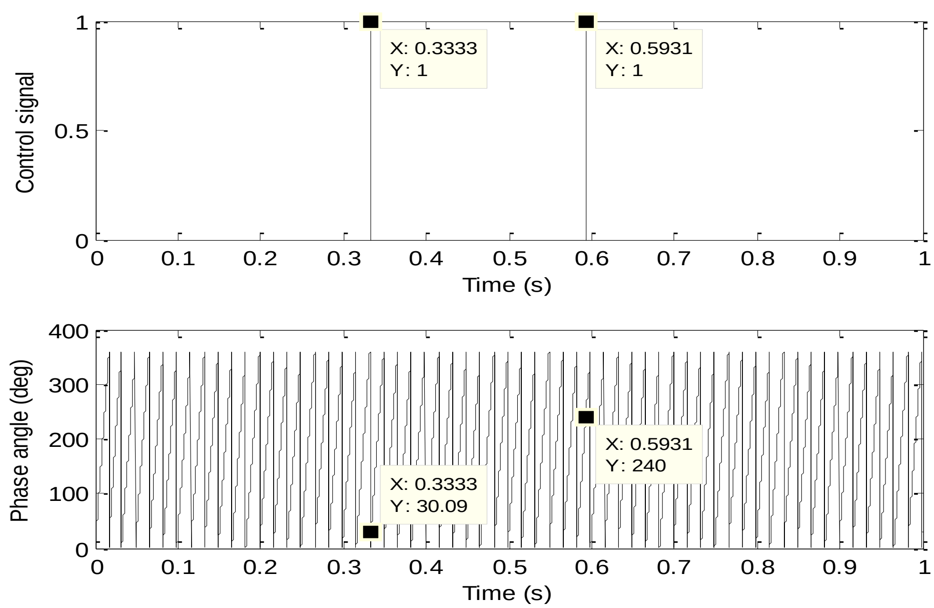

Figure A.1 CB Control signal & Voltage Phase Angle periodic variation

References

[1] H.-T. Tseng and J.-F. Chen, "Bidirectional impedance-type transformer inrush current limiter," *Electric Power Systems Research,* vol. 104, pp. 193-206, 201

[2] Cui, Yu, et al. "A sequential phase energization technique for transformer inrush current reduction-Part I: Simulation and experimental results." *Power Delivery, IEEE Transactions on* 20.2 (2005): 943-949.

[3] J. C. Oliveira, C. E. Tavares, R. Apolonio, A. B. Vasconcellos, and H. S. Bronzeado, "Transformer Controlled Switching to Eliminate Inrush Current - Part I: Theory and Laboratory Validation," in *Transmission & Distribution Conference and Exposition: Latin America, 2006. TDC '06. IEEE/PES*, 2006, pp. 1-5

[4] T. Ghanbari and E. Farjah, "Efficient resonant-type transformer inrush current limiter," *Electric Power Applications, IET,* vol. 6, pp. 429-436, 2012

[5] C. Yu, S. G. Abdulsalam, C. Shiuming, and X. Wilsun, "A sequential phase energization technique for transformer inrush current reduction - Part I: Simulation and experimental results," *Power Delivery, IEEE Transactions on,* vol. 20, pp. 943-949, 2005

[6] Franklin, A.C., Franklin, D.P., "The J&P Transformer Book 11th Edition," *Butterworths*, London, pp 549-641, 1988

[7] V. Molcrette, J. L. Kotny, J. P. Swan, and J. F. Brudny, "Reduction of inrush current in single-phase transformer using virtual air gap technique," *Magnetics, IEEE Transactions on,* vol. 34, pp. 1192-1194, 1998

[8] C. K. Cheng, T. J. Liang, J. F. Chen, S. D. Chen, and W. H. Yang, "Novel approach to reducing the inrush current of a power transformer," *Electric Power Applications, IEE Proceedings -,* vol. 151, pp. 289-295, 2004

[9] J. F. Chen, T. J. Liang, C. K. Cheng, S. D. Chen, R. L. Lin, and W. H. Yang, "Asymmetrical winding configuration to reduce inrush current with appropriate short-circuit current in transformer," *Electric Power Applications, IEE Proceedings -,* vol. 152, pp. 605-611, 2005

[10] J. H. Brunke, “Elimination of transient inrush currents when energizing unloaded power transformers”, Doctoral dissertation no. 12791, ETH, Zurich, 1998

[11] B. Kovan, F. de Leon, D. Czarkowski, Z. Zabar, and L. Birenbaum, "Mitigation of Inrush Currents in Network Transformers by Reducing the Residual Flux With an Ultra-Low-Frequency Power Source," *Power Delivery, IEEE Transactions on,* vol. 26, pp. 1563-1570, 2011

[12] D. I. Taylor, J. D. Law, B. K. Johnson, and N. Fischer, "Single-Phase Transformer Inrush Current Reduction Using Prefluxing," *Power Delivery, IEEE Transactions on,* vol. 27, pp. 245-252, 2012

[13] N. Chiesa, x00F, and H. K. idalen, "Novel Approach for Reducing Transformer Inrush Currents: Laboratory Measurements, Analytical Interpretation and Simulation Studies," *Power Delivery, IEEE Transactions on,* vol. 25, pp. 2609-2616, 2010

[14] C. E. Lin, C. L. Cheng, C. L. Huang, and J. C. Yeh, "Investigation of magnetizing inrush current in transformers. I. Numerical simulation," *Power Delivery, IEEE Transactions on,* vol. 8, pp. 246-254, 1993

[15] H.-T. Tseng and J.-F. Chen, "Bidirectional impedance-type transformer inrush current limiter," *Electric Power Systems Research,* vol. 104, pp. 193-206, 2013

[16] M. Rioual and J. C. Reveret, "Energization of step-up transformers for wind-farms: Modeling and its validation by tests performed on a 10 MW site," in *Power & Energy Society General Meeting, 2009. PES '09. IEEE*, 2009, pp. 1-7

[17] Husianycia, Yoni, and M. Rioual. "Determination of the residual fluxes when de-energizing a power transformer/comparison with on-site tests." *Power Engineering Society General Meeting, 2005. IEEE*. IEEE, 2005.

[18] M. Rioual and B. Bernin, "Impact of the representation of upstream network on the energization of a 340 MVA transformer: modeling and its validation by on site tests"

[19] J. H. Brunke and K. J. Frohlich, "Elimination of transformer inrush currents by controlled switching. I. Theoretical considerations," *Power Delivery, IEEE Transactions on,* vol. 16, pp. 276-280, 2001.

[20] J. H. Brunke and K. J. Frohlich, "Elimination of transformer inrush currents by controlled switching. II. Application and performance considerations," *Power Delivery, IEEE Transactions on,* vol. 16, pp. 281-285, 2001

[21] Stephen J. Chapman, "Electric Machinery Fundamentals", Fourth Edition, McGrawhill Higher Education

[22] Blume, L.F., et al, "Transformer Magnetizing Inrush Currents and Influence on System Operation", *AIEE Transactions,* vol.63, pp 366-375, 1944

[23] Westinghouse, "Applied Protective Relaying", *Westinghouse Electric Corp.,* United States Library of Congress card no. 76-8060, pp 8-2, 8-5, 1976

[24] Moraw, G., et al, "Point on Wave Controlled Switching of High Voltage Circuit Breakers", *CIGRE paper 13-02, pp 1-6*, 28 August-3 September 1988

[25] Richard, N., and N. Szylowicz. "Comparison between a permeance network model and a 2D finite element model for the inrush current computation in a three phase transformer." *Magnetics, IEEE Transactions on* 30.5 (1994): 3232-3235.

[26] De Leon, Francisco, and Adam Semlyen. "Reduced order model for transformer transients." *Power Delivery, IEEE Transactions on* 7.1 (1992): 361-369.

[27] Yacamini, Rua, and H. Bronzeado. "Transformer inrush calculations using a coupled electromagnetic model." *IEE Proceedings-Science, Measurement and Technology* 141.6 (1994): 491-498.

[28] Chuanli, Zhang, and et al. "A new approach to detect transformer inrush current by applying wavelet transform." *Power System Technology, 1998. Proceedings. POWERCON'98. 1998 International Conference on*. Vol. 2. IEEE, 1998.

[29] Mao, Peilin L., and Raj K. Aggarwal. "A novel approach to the classification of the transient phenomena in power transformers using combined wavelet transform and neural network." *Power Delivery, IEEE Transactions on* 16.4 (2001): 654-660.

[30] Li, Qi, and D. T. W. Chan. "Investigation of transformer inrush current using a dyadic wavelet." *Energy Management and Power Delivery, 1998. Proceedings of EMPD'98. 1998 International Conference on*. Vol. 2. IEEE, 1998.

[31] Documentation on Three-Phase Transformer (Two Windings), MATLAB R2013a, http://www.mathworks.com/help/physmod/sps/powersys/ref/threephasetransformertwowindings.html

[32] Documentation on Three phase three limb core type two winding transformer, MATLAB 2013a http://www.mathworks.com/help/physmod/sps/examples/three-phase-three-limb-core-type-two-winding-transformer.html?searchHighlight=core%20type%20transformer

[33] "Assessment of approaches to minimize the impact of energizing power transformers of a wind park", Hydro Quebec Broadcast, November 2013

[34] Documentation on Saturable Transformer, MATLAB 2013a, http://www.mathworks.com/help/physmod/sps/powersys/ref/saturabletransformer.html